Morphological abnormalities of planktonic foraminiferal tests in the SW pacific ocean over the last 550ky

Nicoletta Mancin, Kate Darling

PII: S0377-8398(15)30002-5
DOI: doi: 10.1016/j.marmicro.2015.08.003
Reference: MARMIC 1575

To appear in: *Marine Micropaleontology*

Received date: 16 February 2015
Revised date: 25 June 2015
Accepted date: 21 August 2015

Please cite this article as: Mancin, Nicoletta, Darling, Kate, Morphological abnormalities of planktonic foraminiferal tests in the SW pacific ocean over the last 550ky, *Marine Micropaleontology* (2015), doi: 10.1016/j.marmicro.2015.08.003

Morphological abnormalities of planktonic foraminiferal tests in the SW Pacific Ocean over the last 550ky

Nicoletta Mancin[1], Kate Darling[2&3]

[1] Department of Earth and Environment Sciences, University of Pavia, Italy, nicoletta.mancin@unipv.it

[2]School of GeoSciences, University of Edinburgh, Edinburgh EH9 3FE, UK

[3]School of Geography and GeoSciences, University of St Andrews, Fife, KY16 9AL, UK,

kate.darling@ed.ac.uk

Corresponding author:

Dr. Nicoletta Mancin

Department of Earth and Environment Sciences, University of Pavia

via Ferrata 9, 27100 Pavia, Italy.

e-mail: nicoletta.mancin@unipv.it

Phone: 00390382985894

Fax: 00390382985890

Abstract

The paper focuses on the occurrence of morphologically abnormal specimens of planktonic foraminifera observed over the last 550ky in IMAGES core MD 97-2114 (East of New Zealand, SW Pacific). Abnormal tests occurred throughout the entire record in all the morphospecies characterising the assemblages but were relatively rare, with percentages not exceeding 1.5% of the total assemblage. No mass abnormality events were found. A range of malformations were observed from slight deformity with smaller or overdeveloped chambers to more severe deformity, with misplaced chambers, distorted spirals or double tests forming twinned individuals. They exhibited several different categories of morphological abnormalities, even within the same sample. Test abnormalities were most abundant in the morphospecies *Globorotalia inflata*, *Globigerina bulloides* and *Orbulina universa* and were characterised by a long-term decreasing trend up core with an alternating % abundance pattern at the glacial to interglacial scale between MIS 14 to MIS 8, recording the highest percentages during the interglacials. Normalised total abundance and abnormal abundance curves co-varied very closely for *G. bulloides* and *O. universa*, but for *G. inflata* two opposing excursions were observed during MIS 13 and 6 which may be linked to water column states. Although abnormal numbers were proportionately low, there appears to be a "natural" background number of malformations in the *G. inflata* population through time. There was no relationship between volcanic ash production and test abnormalities.

Keywords: planktonic foraminifera; abnormal test; environmental stressors; Pleistocene, SW Pacific

1. Introduction

Morphological abnormalities of benthic foraminiferal tests have long been documented and various hypothesis relating to either natural ecological causes or human activities have been proposed to explain their occurrence (e.g. Geslin, et al., 2000 and references therein). Natural causes include environmental stressors such as wide fluctuations in salinity (e.g. Stouff et al., 1999; Debenay et al., 2001; Almogi-Labin et al., 1992; Alve, 1995; Ballent and Carignano, 2008; Nigam et al., 2008), water acidification (e.g. Geslin et al., 2002; Le Cadre et al., 2003; Wall-Palmer et al., 2011; Haynert and Schönfeld, 2014), oxygen depletion (e.g. Debenay et al., 2009; Luciani et al., 2010; Geslin et al., 2014), increased terrigenous input (Omaña et al., 2012), nutrification (e.g. Rossignol et al., 2011) and hydrodynamic damages (Stouff et al, 1999; Geslin et al., 2000). Morphological abnormalities relating to human impact on the marine environment are associated mainly with pollution by heavy metals (e.g. Alve, 1991 a and b; 1995; Yanko et al., 1994; 1998; Geslin et al., 2000; 2002; Le Cadre and Debenay, 2006; Frontalini and Coccioni, 2008; 2011; Armynot du Châtelet and Debenay, 2010; Aloulou et al., 2012; Melis and Covelli, 2013) and organic matter produced by eutrophication (Burone et al. 2006). Moreover, many of the proposed natural and anthropogenic causes have been simulated and quantified during the last decade using a range of laboratory experiments and field investigations to identify the specific factors responsible for causing the abnormalities (e.g. Le Cadre et al., 2003; Le Cadre and Debenay, 2006; Nigam et al., 2008; Linshy et al., 2013; Geslin et al., 2014; Haynert and Schönfeld, 2014).

Similar data are largely missing from the literature for the planktonic foraminifera. It is quite curious that test malformations in planktonic foraminifera are rarely documented, even though

they clearly occur in the modern assemblage (personal observation). The few reports of planktonic species displaying test malformations spans a wide range of time and are mostly derived from the fossil record (e.g. Coccioni and Luciani, 2006; Luciani et al. 2010; Rossignol et al., 2011; Omaña et al., 2012; Weinkauf et al., 2014). Malformations and aberrant morphologies have been observed in extinct Cretaceous morphospecies from the Southern Mediterranean region (Verga and Premoli Silva, 2002; Coccioni and Luciani, 2006) and Mexico (Omaña et al., 2012), in middle Eocene subbottinids from Northern Italy (Luciani et al., 2010) and in the Miocene species *Mutabella mirabilis* from the tropical Pacific, Indian and Atlantic Oceans (Pearson et al., 2001). Malformed specimens of the modern morphospecies *Orbulina universa* and *Globorotalia scitula* have also been reported in Pleistocene cores from the Arabian Sea (Rossignol et al. 2011) and Eastern Mediterranean Sea (Weinkauf et al., 2014). Interestingly, test "abnormalities" have been reported in planktonic foraminifera during growth and survival studies in laboratory culture (Bijma et al., 1990), but these appeared more frequently in more normal than extreme conditions. However, the test "abnormalities" described are commonly associated with the mature tests of the morphospecies studied, indicating that at the extremes of the culture environmental conditions less abnormalities occur because the individuals do not reach maturity. There was no indication that these extreme conditions induced the formation of other aberrant abnormalities.

The natural causes hypothesised to explain the occurrence of the planktonic test abnormalities are vague and speculative, invoking an unusually high level of intraspecific variability in chamber shape and arrangement, aperture position and test ornaments (Pearson et al. 2001; Verga and Premoli Silva, 2002) or the combined interplay of different stressor events. These range from the development of oxygen-depleted conditions in the water column (Luciani et al., 2010), sometimes combined with nutrient injections into the photic layer in response to

monsoon activity (Rossignol et al., 2011), to the extremely stressful conditions (rapid and extreme climate fluctuations, sea- level fluctuations, increased terrigenous input and intense volcanism) developing near the K/P boundary (Coccioni and Luciani, 2006, Omaña et al., 2012). However, since the construction of a single chamber requires only a few hours to complete, test malformations may result from highly transient variations in local environmental conditions. They may not necessarily reflect widespread environmental stressors acting on broad time scales, making potential causes very difficult to identify.

In spite of numerous papers dealing mostly with pollution induced morphological abnormalities in benthic foraminiferal tests (e.g. Geslin, 2000; Armynot du Châtelet and Debenay, 2010; Frontalini and Coccioni, 2011; Aloulou et al., 2012), the precise mechanism by which tests develop growth malformations is still unknown. Aberrant morphologies arise when the growth plan of the test is disrupted, producing an abnormal shape compared to the expected morphology developed by the morphospecies within the same population. It is thought that the morphological abnormalities are induced by the stressor interfering with the cytoskeleton assembly which lays down the template for a new chamber (Murray, 2006). It is highly likely that several different biological mechanisms are responsible for producing the range of test abnormalities observed in shallow-water benthic foraminifera. The origin of abnormal twinned or double tests of *Ammonia tepida* and *Elphidium crispum* for example, has been explained as being possibly related to early ontogenetic perturbations in the production and completion of megalospheric juvenile specimens produced during multiple fission (Stouff et al., 1999). However, the possible mechanism producing test abnormalities has never been explained in other studies.

In order to test the potential significance of abnormalities within planktonic foraminiferal assemblages, we have evaluated the number and character of abnormal planktonic specimens found within a Pleistocene sediment core from the SW Pacific Ocean

(core IMAGES MD 97-2114, East of New Zealand) and compared their occurrence with a detailed framework of paleo-environmental information generated from the same core over the last 550ky. We have discussed these data in the light of detailed morphological analyses conducted using Scanning Electron Microscopy (SEM) and have produced a descriptive classification of the morphological abnormalities found within the planktonic foraminiferal assemblages. We have further discussed the significance of our observations with respect to the possible environmental stressor(s) which occurred during the last 550 ky, East of New Zealand.

2. Materials and methods

2.1. Core

The Site IMAGES MD 97-2114 (42°22'27"S; 171°20'42"W) was cored at a water depth of 1936 m on the northern side of the Chatham Rise, East of New Zealand (Fig. 1).The modern oceanography of the surrounding region (Fig. 1) is summarized by Hayward et al. (2012 and references therein). The core MD 97-2114 (ca. 28m) is mostly carbonate pelagic and hemipelagic biogenic mud (Lupi, 2009; Lupi et al., 2008) intercalated with micro- and macroscopic tephra layers (Venuti et al., 2007). The age model documents a continuous sedimentary record of the past 1.07 My, with an average accumulation rate of ca. 2.6 cm/ky (Cobianchi et al., 2012 and references therein). The section described in this study (ca. 16m) covers the last 550 ky and contains at least 11 tephra layers used for dating the core (Mancin et al., 2015 and references therein).

For the last ten years, the core used in this study has been extensively investigated for bio-chronostratigraphical, paleoecological, paleoclimatical and paleoceanographical purposes allowing a detailed chronological and paleoenvironmental framework to be reconstructed (e.g.

Schaefer et al., 2005; Crundwell et al., 2008; Lupi et al., 2008; Cobianchi et al, 2012; 2015; Hayward et al, 2012; Mancin et al., 2013; 2015). It could be considered the "perfect material" on which to carry out the first malformation study on planktonic foraminifera.

2.2. Sample processing

130 sediment samples (every 10 cm = ca. 4 ky) were prepared following standard procedures. Approximately 3cm^3 of dried sediment was washed and sieved through two sieves (63μm and 150μm) and residues were dried in an oven at 40°C. Approximately 300 planktonic foraminifera were counted in random aliquots of both the 63-150μm and >150 μm fractions to obtain census counts of the more common morphospecies. Though the smaller-size planktonic foraminifera are more difficult to taxonomically determine and time-consuming to count (Kucera, 2007), the smaller fraction (63-150μm) of each sample was quantitatively characterised to avoid missing potentially meaningful data (e.g. the species *Turborotalita quinqueloba*, *Globigerinita glutinata* and *Neogloboquadrina pachyderma*).

In order to quantify the total abundance of planktonic foraminifera displaying test abnormalities, the whole >150 μm fraction of each sample was counted (Table A, on-line supplementary data). Percentages were then calculated by comparing the number of abnormal individuals in the whole sample with the expected total number of planktonic specimens in the sample, based on the extrapolation of a counted split. All abnormal specimens identified (over 1800) were picked and stored on slides for taxonomic characterisation at morphospecies level where possible. Assemblage and abnormal specimen counts are recorded in Table A (on-line supplementary data).

2.3. Scanning Electron Microscope (SEM) Imaging

Representative specimens of the "normal" assemblage and selected abnormal specimens (ca. 150) were mounted on stubs using carbon conductive adhesive tape and gold-coated for analyses by SEM imaging at the CiSRIC-Arvedi Laboratory. The SEM (Tescan FESEM, series Mira 3XMU) observations were made with increasing magnification, at 15 mm working distance, using an accelerating voltage of 15 kV.

2.4. Statistical analysis

Percentage curves smoothed on 5 samples were normalized to facilitate comparison of total abnormal specimen curves against total specimen curves. Data were normalized using the software Microsoft Office Excel 2010 through the function *n (normalized value)= (x-a)/y* where *x* is the value to be normalized; *a* is the calculated arithmetic average of the considered distribution smoothed on 5 samples and *y* is the calculated standard deviation of the same distribution. A regression analysis was also performed on the obtained normalized curve; for each x-y plot the linear correlation coefficient of Pearson (r) was calculated.

2.5. Taxonomy and planktonic indexes

Planktonic foraminiferal taxonomy follows the works of Hayward (1983), Hemleben et al. (1989) with additional updates from Darling and Wade (2008) and Morard et al. (2011). Extant species of planktonic foraminifera are typically grouped into five main assemblages (bio-province index assemblages) that characterise and define the tropical, subtropical, temperate, subpolar and polar provinces (Bè and Tolderlund, 1971). An understanding of the environmental factors controlling the spatial and temporal distribution of the modern species facilitates the reconstruction of the state and variation of environments in the recent past. Using this perspective, the distribution/abundance curves for the planktonic bio-province index assemblages were determined (e.g. Kucera et al., 2005 and references therein) to

ascertain the variability in temperature and nutrients in surface waters at the IMAGES site during the last 550 ky. The morphospecies ecological preferences are summarized in Table 1. Tropical-subtropical, temperate and polar-subpolar indexes were produced as a guide to sea surface temperature (SST) variation and oligotrophic and eutrophic indexes were produced as a guide to surface nutrient availability.

3. Results

3.1. The planktonic foraminiferal assemblage

The planktonic foraminiferal assemblages are quite diverse, abundant and generally well preserved throughout the entire record (Figs 2A-B; Plate 1). A total of ca. 43 morphospecies were identified in the >150μm and 63-150μm fractions (Table A, Supplementary data). The most common and abundant morphospecies recorded in the >150μm fraction, are *Globorotalia inflata* Type I (recently renamed *Globoconella inflata* and divided into two Types, I and II respectively, by Morard et al., 2011) (mean relative abundance (MRA) 35%; range 20% - 72%), *Globigerina bulloides* (MRA 25%; range 0 - 60%), *Globorotalia truncatulinoides*-left (MRA 8%; range 2- 20%) and *Orbulina universa* (MRA 8%; range 0 - 25%). Less abundant morphospecies of the larger fraction (MRA <5%) are *G. inflata* Type II (*sensu* Morard et al. 2011), *G. trucatulinoides*-right, *Globorotalia crassaformis*, *Neogloboquadrina dutertrei*, *Neogloboquadrina incompta* and the spinose genus *Globigerinoides*. Important components of the smaller fraction assemblages are *Turborotalita quinqueloba* (MRA 30%; range 18 - 60%), *Globigerinita glutinata* (MRA 25%; range 10 - 50%), *Globigerina falconensis* (MRA 5%; range 2 - 20%), *N. incompta* (MRA 15%; range 5 - 30%) and *Neogloboquadrina pachyderma* (MRA 1%; range 0 - 9%). The

remaining planktonic taxa occurred in very low abundances (MRA <3%) with discontinuous distributions (Table A, supplementary data).

3.2. Assemblage abnormalities

Determining what constitutes an abnormality is quite subjective when determining the limit between normal and abnormal morphology (Geslin, et al., 2000; Murray, 2006). With this proviso, authors have assessed test abnormalities by comparison with recognised morphospecies *norms* described within the literature. The total number of abnormal specimens found within each sediment sample is shown in Fig 3. Abnormal tests were observed throughout the entire record in all the morphospecies characterising the assemblages, but were found to be most abundant in the morphospecies *G. inflata*, *G. bulloides* and *O. universa* (Fig. 3). The remaining morphospecies exhibited very low abnormalities with discontinuous distributions (Table A – Supplementary data).

The morphological abnormalities observed were wide ranging and diverse (Plates 2-4). Abnormal tests displayed different degrees of malformation, ranging from slight deformity with smaller or overdeveloped chambers (e.g. Plate 2, images 4 and 8) to more severe deformity, with chambers in the wrong place (e.g. Pl. 2, image 3), distorted spirals or double tests forming twinned individuals (e.g. Pl. 2, images 9,10, 19). Based on observations derived from analysis of over 1800 abnormal specimens identified within the sediment samples, abnormalities were grouped into nine informal categories (labelled A to I). Similar subdivisions were previously devised by Geslin et al. (2000) for living benthic foraminifera. The categories for the planktonic foraminifera are illustrated in Plate 5. They are: **A)** tests with abnormal additional chamber(s) or protuberance(s); **B)** tests with abnormally protruding chamber(s); **C)** tests with abnormal chamber morphology; **D)** tests with abnormal chamber size (reduced or over-developed chambers); **E)** tests with distorted chamber arrangement; **F)**

twinned tests; **G)** test with abnormal opening(s); **H)** test with a complex shape displaying several categories of abnormalities and **I)** test with traces of regeneration. The classification of all abnormal specimens found in this study are shown in Table B (Supplementary data).

Among the three most abundant morphospecies displaying test malformations (*G. inflata, G. bulloides* and *O. universa*), both *G. inflata* and *G. bulloides* exhibit several different categories of morphological abnormalities, even within the same sample (Table B, Supplementary data). The majority of the abnormalities corresponds to category A (abnormal additional chambers or protuberances), with less abundance observed in categories C (abnormal chamber morphology), D (abnormal chamber size) and G (abnormal openings). The remaining categories (B, H, I, E and F, Plate 5) are much less represented (Table B-supplementary data). *O. universa* presents a very different pattern, and predominantly exhibits abnormal tests belonging to category D. These morphologies closely resemble the morphologies of the morphospecies *Orbulina suturalis* and *Orbulina bilobata* (Kennett and Srinivasan, 1983; Pl. 3 images 14-20; Table B, Supplementary data), which may in reality represent malformed *O. universa* in recent ecosystems. Interestingly, malformations due to mechanical damage of the test followed by regeneration (category I , plate 5) are very rare throughout the core, even though they have highly recognisable characteristic features, as irregular margins of crushed, repaired chambers and/or presence of scars (e.g. Plate 2, 11 and 11a). None of the recognized categories of abnormality seems to prevail in particular glacial or interglacial stages (Table B-supplementary data).

3.3. Abnormalities through time

The total number of abnormal tests and the total abundance curves for planktonic specimens are shown in Fig. 3. From these values, the total % abundance of abnormal specimens has been calculated together with the individual % abundance values for *G. inflata*,

G. bulloides and *O. universa*, the morphospecies which exhibit the majority of the test abnormalities (Fig. 4). These curves are compared with the $\delta^{18}O$ record from both the IMAGES core (Cobianchi et al., 2012; this study) and the standard benthic $\delta^{18}O$ stack LR04 of Lisiecki and Raymo (2005), to determine whether there is any link between incidence of abnormality and environmental change through time. Abnormal specimens were found to be relatively rare, with percentages varying from 0 to 1.38% of the total planktonic foraminiferal assemblage (Fig. 4; Table A, Supplementary data). In general, the % abnormalities are characterised by a long-term decreasing trend up core. They exhibit an interesting alternating abundance/distribution pattern at the glacial/interglacial scale between MIS 14 to MIS 8, recording the highest percentages during the interglacials MIS 13, MIS 11 and MIS 9. Between MIS 8 and MIS 5 the incidence of abnormal specimens is low, but a slight increase in number is observed between MIS 4 and MIS 1. The trends in abnormal specimens through time are overwhelmingly governed by the trends observed in *G. inflata* (Fig. 4). However, more localised peaks are observed for abnormal specimens of *G. bulloides* at the MIS 9/10 boundary and MIS 3 and for *O. universa* at MIS 13 and MIS 11 (Fig. 4; Table A, Supplementary data).

The percentage curves of abnormal tests, *G. inflata* ab, *G. bulloides* ab and *O. universa* ab and the correspondent absolute abundance curves were normalized (see methods) in Fig. 5 to illustrate whether trends in abnormality deviate from the trends in foraminiferal abundance through time. In general, the two total planktonics curves co-vary closely for most of the record with two possible exceptions during MIS 6 and MIS 13 (Fig. 5, MIN and MAX arrows). The curves for both *G. bulloides* ab *vs G. bulloides* and *O. universa* ab *vs O. universa* show a surprisingly high correlation between these independent data (r values of 0.76 and 0.60, respectively), indicating that there is a relatively constant percentage of abnormal specimens throughout both the glacial and interglacial stages. However, the normalised

curves for *G. inflata* ab *vs G. inflata* (Fig. 5) indicate that this is not always the case for *G. inflata* (r = 0,48). Not only does it dominate the abnormal foraminiferal assemblage, but the offsets observed in the normalized total abundance curves during MIS 13 (interglacial) and MIS 6 (glacial, Fig. 5, arrows) are primarily replicated in the *G. inflata* ab *vs G. inflata* curve, indicating that *G. inflata* is the morphospecies responsible for the offsets in the total abundance curve.

3.4. Ecological setting through time

Because the distribution and abundance of planktonic morphospecies is strongly correlated to surface water properties (e.g. Kucera, 2007 and references therein), the taxa shown in Fig 2A and 2B were grouped on the basis of their ecological affinities (Table 1) into ecological index assemblages that were used to reconstruct possible sea-surface conditions (temperature and nutrients) throughout the last 550 ky (see methods; Fig. 6). Kucera (2007) also proposed salinity as a third controlling factor, but since the core site only experienced open ocean conditions (Schlitzer, 2012; http//odv.awi.de), it is thought that salinity is unlikely to be a controlling factor determining the abundance and distribution of the planktonic assemblages. The paleo-ecological indexes were constructed using both the >150μm and 63-150μm fractions, to investigate the variation in the abnormal specimen percentages of *G. inflata*, *G. bulloides* and *O. universa* (Fig. 5) and determine whether specific environmental changes could be linked to the anomalous offset in *G. inflata* abnormality observed during interglacial MIS 13 (increase) and glacial MIS 6 (decrease). The offset observed in the *G. inflata* curve during MIS 8 is due to a single outlier and is most likely an artefact. Also, the offset observed at the MIS 14/13 boundary is most likely a result of very low numbers of *G. inflata* in both data sets.

All paleo-ecological index assemblages show strong cyclicity and they were dominated by temperate to cool water taxa throughout (Fig. 6). Interestingly, the curve of the temperate taxa (>150µm) is a perfect mirror image of the polar-subpolar taxa curve (>150 µm) due to the alternation between *G. inflata* and *G. bulloides* as they cyclically dominate the transitional to polar-subpolar assemblages (Figs. 2A and 2B). Since MIS 8 (ca. 300 ky) there was a dominant trend within the small polar-subpolar taxa plateauing within MIS 6, indicating increased cooling in surface waters (Fig. 6). In parallel, temperate to tropical-subtropical indexes decreased accompanied by a reduction in the average oligotrophic indexes, indicating increasing eutrophication. On the glacial/interglacial scale, cooler glacial intervals were characterised by an increase of polar-subpolar and eutrophic taxa, while during the warmest interglacials, a slight increase of tropical-subtropical and oligotrophic indexes can be recognised (Figs. 2A-B and 6).

With this ecological perspective, it is possible to identify the water conditions prevailing at the times of peak production of abnormal tests (Fig. 4). The % abnormal *G. bulloides* peaks occur at the MIS 9/10 boundary and MIS 3 which correspond to strong peaks in their maximum relative abundance in the sediment (Fig 2A). The peak at the MIS 9/10 boundary occurred prior to the strong increased cooling trend indicated by the small polar-subpolar taxa (Fig. 6A), but is co-incident with the nutrient peak observed at the MIS 9/10 boundary (Fig. 6B). The % abnormal *O. universa* peaks occur within the interglacials MIS 11 and MIS 13 (Fig. 4) which correspond to increased warming and lower nutrient levels in the water column. However, in both these morphospecies, their abnormality peaks are strongly related to their test abundance during these events (Fig. 5). Unlike *G. bulloides* and *O. universa*, the dominant morphospecies *G. inflata* does not always exhibit a constant relationship between abnormality peaks and test abundance (Fig 5). As mentioned above, it exhibits a decoupling of abundance and abnormality at times, particularly during interglacial

MIS 13 (increase; Fig. 5; arrow MAX) and glacial MIS 6 (decrease; Fig. 5; arrow MIN). Examination of the $\delta^{18}O$ record and environmental indexes shows that although MIS 13 was a relatively cool interglacial compared with MIS 11 and 9, it had by far the least number of polar-subpolar taxa in the core assemblages. In addition, the presence of the deep-dweller morphospecies *G. scitula* and *G. hirsuta* in the assemblage (Fig. 2B) may indicate there was a structural difference in the water column during MIS 13 compared with the interglacials MIS 11 and 9, where *G. inflata* abnormality peaks and test abundance closely track one another (Fig 5). The glacial MIS 6 represents the height of the cooling trend in increasingly eutrophic waters (Fig. 6).

4. Discussion

4.1. Abnormality within planktonic foraminiferal populations

In her review, Geslin et al. (2000) provided a classification of test abnormalities exhibited by living benthic foraminifera on the basis of recurrent morphologies without regard to their origins and causes. Following a similar approach, we described and SEM imaged the different categories of morphological abnormalities exhibited by Pleistocene planktonic foraminifera from the SW Pacific (Plates 2-5). Interestingly, our data show that comparable test abnormalities occur in both planktonic and benthic foraminifera, even though the planktonics are suspended freely in the water column rather than inhabiting the sedimentary habitats of the benthos. This suggests that similar test abnormalities occur, regardless of potentially different stressing conditions, due to the limited test constructions and forms that are physically possible. The shape and arrangement of foraminiferal chambers is primarily genetically controlled, but the cell components play a physical role in constructing the test. The question of whether planktonic foraminiferal cells make functional adaptations to test

shape in response to different environmental conditions (ecophenotypes) is still largely unknown. However, if environmental stressors are outside their normal adaptive range, it is quite possible that foraminiferal cell behavior would be affected, producing test abnormality. Test malformations could potentially be also induced by genetic mutation, which would depend on whether the stressor affected reproduction and/or DNA replication. We have no data to discriminate between the influence of an external stressor on foraminiferal cell behavior or on genetic mutation, but genetic mutation would seem less probable. We observed that the test malformations occurred simultaneously in all the morphospecies studied within the same sample. If a mutation was responsible, it would have to be assumed that the same genetic mutation contemporaneously affected all the morphospecies exhibiting test abnormalities, even though they are genetically diverse and ecologically divergent.

The question remaining to be answered is whether there is a constant background number of "natural" malformations in planktonic foraminifers through time or whether the percentage varies in response to the intensity of the stressors. Further, if the percentage does vary, are the variations associated with specific morphospecies and are any particular malformations related to the type and intensity of identifiable stressors?

4.2. Percentage abnormality down core

In the literature, the percentage of abnormal benthic foraminiferal specimens is reported to be highly variable within living assemblages coming from both stressed and normal environments (from 1-3% to over 40%; Stouff, 1999; Yanko et al., 1998; Coccioni, 2000; Geslin et al., 2002; Frontalini and Coccioni, 2008). For this reason some authors tentatively proposed the limit of 1% above which the percentage of malformed tests can be considered "abnormal" (e.g. Alve, 1991a,b; Stouff et al, 1999; Geslin, et al., 2000). In our samples, specimens exhibited abnormalities mostly below 0.5% and more rarely up to 1.38%

of the assemblage, close but sometimes above the 1% limit (Fig. 4; Table A- Supplementary data). However, it cannot be assumed that benthic abnormality values will apply to the planktonics. We do however believe it reasonable to suggest that the range of values for the malformed specimens in the IMAGES core is representative for values of test abnormalities associated with planktonic foraminiferal populations in natural conditions. Nevertheless, it is difficult to judge what should be considered as a "normal" background level.

In the studied core the percentage of abnormal tests was not constant, but showed a clear variability over time; the values ranged between 0 and 1.38% (Fig. 4; Table A-Supplementary data), with only 3 intervals when the percentage rose above 1% within a long-term decreasing trend up core. The highest percentages were observed during the interglacial MIS 13, MIS 11 and MIS 9 and then decreased progressively up core with a further slight increase during MIS 3 into 2The total abundance curve shows cyclical variability with no consistent relationship with glacial/interglacial (G/I) cyclicity, but it does exhibit a substantial long-term increasing trend up core (particularly since MIS 8) as opposed to the downward trend in the percentage abnormal curve. That is, with increasing numbers of foraminifers in the sediment sample, the percentage of abnormal specimens decreases up core (Figs 3 and 4). This downward trend in the total % abnormality curve is not the result of an alternation in morphospecies, since *G. inflata* clearly represents the majority of abnormal specimens in the >150µm fraction (Fig. 3, Table A-supplementary data). The *G. inflata* abundance curve (Fig 3) indicates that there was a slight increasing trend in *G. inflata* abundance yet there was a reducing trend in the percentage of abnormal *G. inflata* (Fig. 4). This suggests that the low abnormality levels observed in *G. inflata* between MIS 8 and MIS 3 may represent a "normal" background level of abnormality in *G. inflata* and that the peaks observed earlier between MIS 13 - 9 represent elevated levels, potentially induced by stressors within the environment. Similar much smaller trends were also observed in *G. bulloides* and *O. universa* (Fig. 3).

The increased percentage of abnormal specimens of *G. inflata* is cyclical and mostly associated with the warmer interglacials prior to MIS 8 (Fig. 4). The smaller peaks in abnormality observed in the *G. bulloides* and *O. universa* curves were more sporadic and discrete (Fig. 4). The normalized percentage curves in figure 5 show that they mainly co-vary with a few notable exceptions. Even though percentages of abnormal specimens are low, the curves for both *G. bulloides* and *O. universa* show a surprisingly high correlation, suggesting that they have a more or less constant percentage of abnormal specimens, independent of glacial/interglacial changes. However, in *G. inflata*, the normalized curves largely co-vary during interglacials with the exception of MIS 13, where there is a large and opposite excursion indicating a proportionately greater percentage of abnormal specimens of *G. inflata* in the sediments during interglacial MIS 13. Further, there is also a contrasting large and opposite excursion during glacial MIS 6, indicating a proportionately lower percentage of abnormal specimens of *G. inflata* in the sediments (Fig. 5).

4.3. Potential stressors

4.3.1. Paleoceanographic ecological conditions

Using the relative abundance curves (Fig 2A and B) and paleoenvironmental indexes (Fig. 6), it is possible to gain an understanding of the paleoenvironmental conditions prevailing when the mismatches in abnormal and abundance curves described above occur. The percentage peak in abnormal specimens of *G. inflata* during MIS 13 coincides with high levels of *G. inflata* Type II, *G. scitula* and *G. hirsuta* in the assemblage. This is quite interesting since *G. inflata* Type II is today specifically associated with eutrophic, mixed subpolar waters (Morard et al, 2011), yet the most eutrophic index morphospecies *G. bulloides* is at its lowest percentage level at this time, which is also consistent with oligotrophic taxa being at their

highest levels (Fig. 6). Further, *G. scitula* and *G. hirsuta* are also both considered oligotrophic indexes and usually inhabit the deep layers of a stratified water column. The assemblages are clearly quite unusual during MIS 13 and are suggestive of a period of constantly alternating mixed and stratified water column modes. By using a combination of these paleoecological indexes (Fig. 6) and evidence from the literature (e.g. Schaefer et al., 2005; Crundwell et al., 2008; Cobianchi et al., 2012; Hayward et al., 2012), it is possible to reconstruct the broad paleoceanographic setting in which *G. inflata* exhibited maximal abnormality (MIS 13; Fig 5; arrow MAX). The moderate increase of tropical-subtropical and oligotrophic indexes during the warmest interglacial MIS 13 can be considered the response of a major influence of the STW inflow and the consequent migration of the STF towards the south with the development of more oligotrophic conditions and an increased stratification in the water column (Fig. 1; Crundwell et al., 2008; Hayward et al., 2012). Alternations in this front migration could explain the increased abnormalities recorded in *G. inflata* during the interglacial MIS13. Since *G. inflata* Type II reached maximal numbers within the *G. inflata* assemblage at this time (Fig. 2B), it is highly likely that the genotype II is the most stressed and the one producing the most abnormal tests. Alternatively, it is important to note that *G. inflata* expanded its geographic range to the southern subpolar waters around the Middle Pleistocene Transition (ca. 700 ky; Morard et al., 2011). This event most likely corresponds to the partitioning of ancestral *G. inflata* into genotypes I and II, where Type II is restricted to Antarctic subpolar waters in the present day. In this study, although the morphology of *G. inflata* specimens has been differentiated as accurately as possible, the resulting relative abundance data of *G. inflata* genotypes appear anomalous and contrary to ecological indexes. This is particularly the case in the oldest section of the core and could indicate that *G. inflata* may not have been fully ecologically differentiated at that time, resulting in a higher degree of test abnormality during a period of low abundance during MIS13.

In contrast to interglacial MIS 13, there was a relative fall in abnormal specimens in the *G. inflata* assemblage during the glacial MIS 6. Eutrophic and polar sub-polar taxa were peaking during MIS 6 (Fig. 6) and *G. inflata* abundances were high (Fig. 3). Both Crundwell et al. (2008) and Hayward et al. (2012) suggested that during extreme glacials such as MIS 6, SST's were slightly cooler (11-14 °C) at the core site, being influenced by cooler and more nutrient-rich waters from the south. Such transitional water could represent the most favourable conditions for *G. inflata*-Type I, minimising the production of abnormal tests (Fig 5; arrow MIN).

4.3.2. Volcanism

Another possible candidate that could act as a natural stressor causing morphological abnormalities could be the explosive volcanism of the Taupo Volcanic zone (TVZ, Fig.1) off the North Island of New Zealand. Such explosive volcanism can cause mass mortality of planktonic organisms or induce test malformations in the whole water column (e.g. Wall-Palmer et al., 2011 and references therein). For the last 1.6 My, the TVZ has been characterized by voluminous eruptions which dispersed abundant volcanic ash widely offshore New Zealand to form micro and macroscopic volcanoclastic layers, mostly made of glass spherules (Alloway et al., 2004; Carter et al., 2004; Venuti et al., 2007; Mancin et al., 2015; Cobianchi et al., 2015). To determine whether an increase of abnormal specimens is associated with the tephra layers, the percentage of abnormal specimens was plotted against the percentage of glass fragments (Fig. 7). There is no significant correlation between the incidence of abnormal specimens, as shown by the very low correlation coefficient (r = 0,001). Therefore we have no evidence that the downfall of volcanic ash has induced test abnormalities in the planktonic assemblages of this study. It is very important to note however, that the sampling intervals in this study have an estimated duration of approximately

4Ky, while single volcanic eruption episodes can occurs within a few years. Lack of correlation between volcanic events and abnormality may therefore only imply that our sampling resolution is too low to detect the impact of transient volcanic activity. To reveal the impact of such potentially short term stressors, it would be necessary to carry out detailed sampling of particularly high resolution possibly laminated sediments, which could be correlated with volcanic tephra. Such records are rare, but should provide the answer to whether repeated explosive volcanism with its associated surface ocean acidification by volcanic gases and ejecta causes mass mortality or induce test malformations of planktonic organisms in the whole water column.

5. Conclusion

The idea of documenting abnormal morphologies in foraminifera has wider implications for helping define patterns of marine biodiversity (and identifying potential times of change or stress), which is relevant to predicting future biodiversity change. The present work reports for the first time the morphological abnormality in an open ocean planktonic foraminiferal test assemblage (>150 μm fraction).

Abnormalities were observed in all morphospecies throughout the entire record (550ky) and were comparable to those observed in benthic assemblages. Abnormal specimens were rare and never exceeded 1.5% of the total assemblage. Different categories of abnormality were found within a single morphospecies and were most abundant in the morphospecies *G. inflata* and in *G. bulloides* and *O. universa*. The trends in total abnormal specimens through time were overwhelmingly governed by the trends observed in *G. inflata*.

Percentage abnormality exhibited an alternating abundance pattern at the glacial/interglacial scale between 550-300ky (MIS14-8), with the highest percentages observed during the warmer interglacials. This was followed by a long-term decreasing trend

in % abnormality up core, concurrent with the highest numbers of specimens per sample, with a further slight increase in abnormality after MIS 3. The period from 300-50ky represent a minimal background level of abnormality for *G. inflata*, *G. bulloides* and *O. universa*. Their independent normalised percentage abnormality and abundance curves demonstrate a surprisingly high correlation, given the low numbers of abnormal specimens. The percentage of abnormal specimens closely tracks abundance throughout both the glacial and interglacial stages with only two possible exceptions. The first is a proportionately low level of abnormality in *G. inflata* during glacial MIS 6, when the core site was influenced by cooler and more nutrient-rich waters. This may have favoured test growth, minimising abnormal test production. The second is a proportionately high level of abnormality in *G. inflata* during glacial MIS 13. Reconstruction of the broad paleoceanographic setting at this time suggest it may have been a period of constantly alternating water column modes, leading to increased abnormal test production.

In conclusion, although abnormal percentages are low, there does appear to be a background number of "natural" malformations in the planktonic foraminiferal population through time, particularly in *G. inflata*. This implies that there may be a 'base line' for background abnormalities in planktonic foraminifera. In *G. inflata*, the percentage of abnormal tests decreased in the most favourable conditions and increased during perturbations of the system. No specific categories of malformations correlated with these events.

No relationship was found between volcanic ash production and test abnormalities and no mass abnormality events were observed during the last 550ky in this region. However, this may be due to lack of resolution and we cannot exclude the possibility that high resolution studies may reveal a relationship between volcanic activity and test malformations in future studies.

Acknowledgements

The authors thank Prof. M. Kucera for some constructive suggestions on abnormal planktonic foraminifera and Prof. W. E. N. Austin for advice on micropaleontological analysis. We also thank Prof. F. Jorissen and two anonymous reviewers for suggestions that have improved this manuscript. We are grateful to the staff of the CiSRIC-Arvedi Laboratory for SEM photos and especially to Dr. E. Basso for her technical assistance. This project was funded by "FAR 2012-2014" grants of the University of Pavia (Italy).

Reference list

Alloway, B., Westgate, J., Pillans, B., Pearce, N., Newham, R., Byrami, m., Aarburg., S., 2004. Stratigraphy, age and correlation of middle Pleistocene silicic tephras in the Auckland region, New Zealand: a prolific distal record of Taupo Volcanic Zone volcanism. New Zealand Journal of Geology and Geophysics, 47, 447-479.

Almogi-Labin, A., Perelis-Grossovicz, L., Raab, M., 1992 –Living *Ammonia* from a hypersaline inland pool, Dead Sea area, Israel. Journal of Foraminiferal Research, 22(3), 257-266.

Aloulou, F., EllEuch, B. Kallen M. 2012. Benthic foraminiferal assemblages as pollution proxiesin the northern coast of Gabes Gulf, Tunisia. Environ. Monit. Assess., 184, 777-795.

Alve, E., 1991a. Benthic foraminifera in sediment cores reflecting heavy metal pollution in Sorf jord, western Norway. Journal of Foraminiferal Research, 21, 1-19.

Alve, E., 1991b. Benthic foraminifera reflecting heavy metal pollution in Sérfiord, western Norway. Journal of Foraminiferal Research, 34, 1641-1652.

Alve, E., 1995. Benthic foraminiferal responses to estuarine pollution: a review. Journal of Foraminiferal Research, 25, 190-203.

Armynot du Châtelet, E., Debenay, J.P. 2010. The anthropogenic impact on the western French coasts as revealed by foraminifera: a review. Revue de Micropaléontologie, 53, 129-137.

Aurahs, R., Treis, Y., Darling, K., Kucera, M. 2011. A revised and phylogenetic concept for the planktonic foraminifer species *Globigerinoides ruber* based on molecular and morphometric evidence. Marine Micropaleontology, 79, 1-14.

Ballent, S.C., Carignano, A.P. 2008. Morphological abnormalities in Late Cretaceous and early Paleocene foraminifer tests (Northern Patagonian, Argentina). Marine Micropaleontology, 67, 288-296.

Bè, A.W. H., Tolderlund, D.S. 1971. Distribution and ecology of planktonic foraminifera. In: Funnell, B.M., Riedel, W.R. (eds), The micropaleontology of oceans. Cambridge University press, 105-150.

Bijma, J., Faber, W.W., Hemleben, C. 1990. Temperature and salinity limits for growth and survival of planktonic foraminifera in laboratory cultures. Journal of Foraminiferal Research, 20(2), 128-148.

Burone, L., Venturini, N., Sprechmann, P., Valente, P., Muniz, P. 2006. Foraminiferal responses to polluted sediments in the Montevideo coastal zone, Uruguay. Marine Pollution Bulletin, 52, 61-73.

Carter, L., Alloway, B., Shane, P., Westgate J., 2004. Deep-ocean record of major late Cenozoic rhyolitic eruptions from New Zealand. New Zealand Journal of Geology and Geophysics, 47, 481-500.

Cobianchi, M., Luciani, V., Lupi, C., Mancin, N., Lirer, F., Pelosi, N., Trattenero, I., Bordiga, M., Hall, I.R., Sprovieri, M., 2012. Pleistocene biogeochemical record in the south-west Pacific Ocean (Images Site MD 97-2114, Chatham Rise. Journal of Quaternary Science (2012), DOI: 10.1002/jqs.2542.

Cobianchi, M., Mancin, N., Lupi, C., Bordiga, M., Bostock, H., 2015. Effects of ocean circulation and volcanic ash-fall on calcite dissolution in bathyal sediments from the SW Pacific Ocean over the last 550 ka. Palaeogeography, Palaeclimatology, Palaeoecology, 429, 72-82, doi:10.1016/j.palaeo.2015.03.045.

Coccioni, R., 2000. Benthic foraminifera as bioindicators of heavy metal pollution – a case study from the Goro Lagoon (Italy). In: Martin, R.E. (Ed.), Environmental

Micropaleontology: the application of microfossils to environmental geology. Kluwer Academic/Plenum Publishers, 71-103.

Coccioni, R., Luciani, V. 2006. *Guembelitria irregularis* bloom at the K/T boundary: morphological abnormalities indicued by impacte-related extreme environmental stress? In: Cockell C., Koeberl C., Gilmour, I (Eds.). Biological processes associated with impact events, Springer, 179-196.

Crundwell, M.P., Scott, G.H., Naish, T., Carter, L., 2008. Glacial-interglacial ocean climate variability from planktonic foraminifera during the Mid-Pleistocene transition in the temperate South West Pacific, ODP Site 1123. Palaeogeography, Palaeoclimatology, Palaeoecology 260, 202-229.

Darling K., Kucera, M., Kroon, D., Wade C.M., 2006. A resolution for the coiling direction paradox in *Neogloboquadrina pachyderma*. Paleoceanography, 21, 1-14.

Darling, K., Wade, C.M. 2008. The genetic diversity of planktonic foraminifera and the global distribution of ribosomal RNA genotypes. Marine Micropaleontology, 67, 216-238.

Debenay, J.P., Geslin, E., Eichler, B.B., Duleba, W., Sylvestre, F., Eichler P. 2001. Foraminiferal assemblages in a hypersaline lagoon, araruma (R.J.) Brazil. Journal of Foraminiferal Research, 31(2), 133-151.

Debenay, J.P., Della Patrona, L., Herbland, A., Goguenheim, H. 2009. The impact of easily oxidized material (EOM) on meiobenthos: foraminifera abnormalities in shrimp ponds of New Caledonia: implications for environment and paleoenvironment survey. Marine Pollution Belletin, 59, 323-335.

Frontalini, F., Coccioni, R., 2008. Benthic foraminifera for heavy metal pollution monitoring: a case study from the central Adriatic Sea coast of Italy. Estuarine, Coastal and Shelf Science, 76, 404-417.

Frontalini, F., Coccioni, R. 2011. Benthic foraminifera as bioindicators of pollution: a review of Italian research over the last three decades. Revue de Micropaléontologie, 54, 115-127.

Geslin, E., Stouff, V., Debenay, J.P., Lesourd, M. 2000. Environmental variation and foraminiferal test abnormalities. In: R.E. Martin (Ed.). Environmental Micropaleontology, vol. 15 of Topics in Geobiology. Kluer Academic, 191-215.

Geslin, E., Debenay, J.P., Duleba, W., Bonetti, C. 2002. Morphological abnormalities of foraminiferal tests in Brazilian environments: comparison between polluted and non-polluted areas. Marine Micropaleontology, 45, 151-168.

Geslin, E., Barras, C., Langlet, D., Nardelli, M.P., Kim, J-H., Bonnin, J., Metzger, E., Jorissen, F.J. 2014. Survival, Reproduction and calcification of three benthic foraminiferal species in response to experimental induced hypoxia. In: H. Kitazato and J.M. Berhnard (Eds). Approaches to study living foraminifera: collection, maintenance and experimentation. Environmental Science and Engineering, doi 10.1007/978-4-431-54388-6_10, Springer Japan.

Haynert, K. Schönfeld, J. 2014. Impact of changing carbonate chemistry, temperature, and salinity on growth and test degradation of the benthic foraminifer *Ammonia aomoriensis*. Journal of Foraminiferal Research, 44(2), 76-89.

Hayward, B.W., 1983. Planktonic foraminifera (Protozoa) in New Zealand waters: a taxonomic review. New Zealand Journal of Zoology, 10, 63-74.

Hayward, B.W., Sabaa A.T., Kolodziej, A., Crundwell. M.P., Steph, S., Scott, G.H., Neil, H.L., Bostock, H.C., Carter, L., Grenfell, H. 2012. Planktic foraminifera-based sea-surface temperature record in the Tasman Sea and history of the Subtropical Front around New Zealand, over the last one million years. Marine Micropaleontology 82-83, 13-27.

Hemleben, C., Spindler, M., Anderson, O.R. 1989. Modern Planktonic Foraminifera. Springer, Berlin, 363 pp.

Kennett, J. P., Srinivasan, M. S. 1983. Neogene Planktonic Foraminifera, a Phylogenetic Atlas (Hutchinson and Ross, Stroudsburg, Pennsylvania, 1983).

Kucera, M. 2007. Planktonic foraminifera as tracers of Past oceanic environments. Development in Marine Geology, 1, 213-261.

Kucera,M., Weinelt, M., Kiefer, T., Pflaumann, U., Hayes, A., Weinelt, M. Chen, M.T., Mix, A.C., Barrows, T.T., Cortijo, E., Duprat, J., Juggins, S., Waelbroeck, C. 2005. Reconstruction of sea-surface temperatures from assemblages of planktonic foraminifera: multi-technique approach based on geographically constrained calibration datasets and its application to glacial Atlantic and Pacific Oceans. Quaternary Science Reviews, 24, 951-998.

Le Cadre, V., Debenay, J.P., Lesourd, M. 2003. Low pH effects on *Ammonia beccarii* test deformation: implications for using test deformations as pollution indicator. Journal of Foraminiferal Research, 33(1), 1-9.

Le Cadre, V., Debenay, J.P. 2006. Morphological and cytological responses of *Ammonia* (Foraminifera) to copper contamination: implication for the use of foraminifera as bioindicators of pollution. Environmental Pollution, 143, 304-317.

Linshy, V.N., Saraswat, R., Kurtarkar, S.R., Nigam, R. 2013. Experiment to decipher the effect of heavy metal cadmium on coastal benthic foraminifer *Pararotalia nipponica* (Asano). Journal of Paleontological Society of India, 58(2), 205-211.

Lisiecki, L.E., Raymo, M.E., 2005. A Pliocene-Pleistocene stack of 57 globally distributed benthic delta O-18 records. Paleoceanography 20, PA1003. http://dx.doi.org/10.1029/2004PA001071.

Luciani, V., Giusberti, L., Agnini, C., Fornaciari, E., Rio, D., Spofforth, D.J.A., Pälike, H. 2010. Ecological and evolutionary response of Tethyan planktonic foraminifera to the middle Eocene climatic optimum (MECO) from the Alano section (NE Italy).

Lupi, C., 2009. Biostratigraphic correlation and paleoceanographic interpretation of Pleistocene calcareous nannofossils from the Subtropical Front to the Antarctic Divergence. Micropaleontology 55, 383-395.

Lupi, C., Luciani, V., Cobianchi, M., 2008. Integrated calcareous nannofossil and planktonic foraminiferal bioevents of the last 1.07Ma: a case study from the East New Zealand Pacific Ocean. Micropaleontology 54, 463-476.

Mancin, N., Hayward, B.W., Trattenero, I., Cobianchi, m., Lupi, C., 2013. Can the morphology of deep-sea benthic foraminifera reveal what caused their extinction during mid-Pleistocene Climate Transition? Marine Micropaleontology, 104, 53-70.

Mancin, N., Basso, E., Lupi C., Cobianchi, M., Hayward, B.W. 2015. The agglutinated foraminifera from the SW Pacific bathyal sediments of the last 550 kyr: relationship with the deposition of tephra layers. Marine Micropaleontology 115, 39-58.

McCave, I.N., Carter, L., Hall, I.R., 2008. Glacial-interglacial changes in water mass structure and flow in the SW Pacific Ocean. Quaternary Science Reviews 27, 1886-1908.

Melis, R., Covelli, S. 2013. Distribution and morphological abnormalities of recent foraminifera in the Marano and Grado Lagoon (North Adriatic Sea, Italy). Mediterranean Marine Science, 14(1), 432-450.

Morard, R., Quillévéré, F., Douady, C.J., de Vergas C., de Gardel-Thoron, T., Escarguel, G. 2011. Worldwide genotyping in the planktonic foraminifer *Globoconella inflata*: implications for life history and paleoceanography. PLoS ONE, 6(10), 1-11.

Murray, J.W., 2006. Ecology and applications of benthic foraminifera. Cambridge University Press, 440 p.

Nigam, R., Kurtar, S.R., Sarawat, R., Linsky, V.N., Rana, S.S. 2008. Response of benthic foraminifera *Rosalina leei*, to different temperature and salinity, under laboratory culture experiment. Journal of the Marine Geological association of the United Kingdom, 88, 699-704.

Omaña, L., Alencàster, G., Torres Hernàndez, J.R., Lopez Doncel, R. 2012. Morphological abnormalities and dwarfism in Maastrichtian foraminifera from the Càrdenas Formation, Valles-San Luis Potosì Platorm, Mexico: evidence of paleoenvironmental stress. Boletìn de Sociedad Geologìca Mexicana, 64 (3), 305-318.

Pearson, P. N., Norris, R. D., and Empson, A. J. 2001. *Mutabella mirabilis* gen. et sp. nov., a Miocene microperforate planktonic foraminifer with an extreme level of intraspecific variability. Journal of Foraminiferal Research, 31(2), 120-132.

Rossignol, L., Eynaud, F., Bourget, J., Zaragosi, S., Fontanier, C., Elloz-Zimmermann, N., Lanfumey, V. 2011. High occrence of *Orbulina suturalis* and "*Praeorbulina*-like specimens" in sediments of the northern Arabian Sea during the Last Glacial Maximum. Marine Micropaleontology, 79, 100-113.

Schaefer, G., Rodger, J.S., Hayward, B.W., Kennett, J.P., Sabaa, A.T., Scott, G.H. 2005. Planktic foraminiferal and sea-surface temperature record during the last 1 Myr across the Subtropical Front, Southwest Pacific. Marine Micropaleontology, 54, 191-212.

Schlitzer, 2012. In: http//odv.awi.de; Ocean Data View (ODV) the software package for the interactive exploration, analysis and visualization of oceanographic and other geo-referenced profile, time-series, trajectory or sequence data. Stouff, V., Debenay, J.P., Lesourd, M., 1999. Origin of double and multiple tests in benthic foraminifera: observations in laboratory cultures. Marine Micropaleontology, 36, 189-204.

Ujiié, Y., de Garidel-Thoron, T., Watanabe, S., Wiebe, P., de Vargas, C. 2010. Coiling dimorphism within a genetic type of planktonic foraminifer *Globorotalia truncatulinoides*. Marine Micropaleontology, 77, 145-153.

Ufkes E., Jansen J.H.F. Brummer, G.J. 1998. Living planktonic foraminifera in the eastern South Atlantic during spring: indicators of water masses, upwelling and Congo (Zaire) River plume. Marine Micropaleontology, 33, 27-53.

Venuti, A., Florindo, F., Michel, E., Hall, I.R., 2007. Magnetic proxy for the deep (Pacific) western boundary current variabilità across the mid-Pleistocene climate transition. Earth and Planetary Science Letters 259, 107-118.

Verga, D., Premoli Silva, I. 200., Early Cretaceous planktonic foraminifera from the Tethys: the genus *Leupoldina*. Cretaceous Research 23(2), 189-212.

Wall-Palmer, D., Jones, M.T., Hart, M.B., Fisher, J.K., Smart, C.W., Hembury, D.J., Palmer, M.R., Fones, G.R. 2011. Explosive volcanism as a cause for mass mortality of pteropods. Marine Geology, 282, 231-239.

Weikauf, M.G., Moller, T., Koch, M.C., Kucera, M. 2014. Disruptive selection and bet-hedging in planktonic foraminifera: shell morphology as predictor of extinctions. Frontiers in Ecology and Evolution, 2 (64), 1-12.

Yanko, V., Kronfeld, J., Flexer, A. 1994. Response of benthic foraminifera to various pollution sources: implications for pollution monitoring. Journal of Foraminiferal Research, 24, 1-17.

Yanko, V., Ahmad, M., Kaminski, M.A. 1998. Morphological deformities of benthic foraminiferal tests in response to pollution by heavy metals: implications for pollution monitoring. Journal of Foraminiferal Research, 28, 177-200.

FIGURE CAPTIONS

Fig. 1. Synthetic map of the area around New Zealand and location of the studied IMAGES site MD 97-2114 and of the Taupo Volcanic Zone (TVZ). The surface oceanography with the relative position of the major water masses, fronts and currents are redrawn and partly modified by Hayward et al. (2012).

Fig. 2A-B. Distribution curves showing the relative abundance of the most common planktonic morphospecies plotted against the $\delta^{18}O$ record from both the studied IMAGES core (Cobianchi et al., 2012) and the standard LR04 (in grey on the left) of Lisiecki and Raymo (2005). Interglacials are shaded. Taxonomic subdivision followed the papers of Darling and Wade (2008) and Morard et al. (2011).

Fig. 3. Distribution curves reporting the total abundance of both abnormal planktonic foraminifera and of abnormal specimens determined for the most common morphospecies (*G. inflata, G. bulloides, O. universa*) plus the combined remainder, counted in the whole >150 μm fraction. Below, the total abundance curves of the species which developed test malformation are also shown. The abundance curves are plotted against the $\delta^{18}O$ records, as in Fig. 2. Interglacials are shaded.

Fig. 4. Distribution curves reporting the percentage of abnormal planktonic foraminifera within the total assemblage and the percentage of abnormal specimens within the most common morphospecies (*G. inflata, G. bulloides, O. universa*) plus the combined remainder.

The abundance curves are plotted against the $\delta^{18}O$ records as in Fig. 2. Interglacials are shaded.

Fig. 5. Comparison of normalised percentage curves of abnormal planktonic foraminifera , *G. inflata* % ab, *G. bulloides* %ab and *O. universa* %ab (red) against their normalised total abundance curves (black; see methods). The curves are plotted against the $\delta^{18}O$ records as in Fig. 2. Note that the percentage curves co-vary for most of the studied record apart from during MIS 13 (arrow MAX) and MIS 6 (arrow MIN). The corresponding x-y plots with the linear coefficient *r* are also imaged below. Interglacials are shaded.

Fig. 6. Abundance patterns of planktonic foraminiferal paleoecological indexes plotted against the $\delta^{18}O$ records as in Fig. 2. See the text for further explanations. Interglacials are shaded.

Fig. 7. Distribution curves showing the percentage of glass fragments recorded in both ODP 1123 and IMAGES MD 97-2114 sites and the percentage of abnormal specimens counted in the whole >150 μm fraction. The curves are plotted against the $\delta^{18}O$ records, as in Fig. 2. Interglacials are shaded; yellow and orange bars mark the position of rhyolitic tephra layers. The corresponding x-y plot with the linear coefficient *r* is also imaged below.

TABLE CAPTION

Table 1. Ecological preferences of the most common morphospecies of modern planktonic foraminifera. Reference papers are indicated as numbers on the right column.

PLATE CAPTIONS

Plate 1

The most common morphospecies of planktonic foraminifera occurring in the core IMAGES MD 97-2114, Chatham Rise (New Zealand).

1: *Globigerina bulloides*, (7,42 meters below sea floor - mbsf). **2a,b:** *Globigerinella aequilateralis* (4,98 mbsf). **3:** *Globigerinoides elongatus* (4,33 mbsf). **4:** *Turborotalita quinqueloba* (4,20 mbsf). **5:** *Orbulina universa* (4,33 mbsf). **6:** *Globigerinita minuta* (0,47 mbsf). **7a,b:** *Globigerinita glutinata* (6,24 mbsf). **8:** *Globorotalia crassaformis* (5,60 mbsf). **9:** *Globorotalia hirsuta* (0 mbsf). **10a,b:** *Globorotalia inflata*, Type II (*sensu* Morard et al., 2011) (4,33 mbsf). **11a,b:** *Globorotalia inflata*, Type I (*sensu* Morard et al., 2011) (0,84 mbsf). **12:** *Globorotalia truncatulinoides* (right) (5,72 mbsf). **13:** *Globorotalia truncatulinoides* (left) (5,72 mbsf). **14:** *Globorotalia scitula* (5,34 mbsf).**15:** *Neogloboquadrina pachyderma* (5,34 mbsf). **16a,b:** *Neogloboquadrina incompta* (5,34 mbsf).

Plate 2

Abnormal specimens of *Globorotalia inflata* throughout the studied record. Note that this morphospecies exhibits various morphological abnormalities, often within the same sample. **1-3:** Specimens with abnormal additional chambers (1,08 mbsf). **4-5:** Specimens with an abnormally protruding chamber (1,21 mbsf). **6-7:** Specimens with chambers characterised by an abnormal morphology (14,46 mbsf). **8:** Abnormal specimen with a chamber reduced in size (1,08 mbsf). **9-10**: Abnormal specimens partly blended to form twinned tests (13,11 mbsf). **11:** Abnormal specimen with traces of test regeneration (0,47 mbsf); **a)** detail showing the repaired chamber with the presence of a marked scar. **12-16:** Specimens with abnormal

subsidiary openings sometimes covered by a bulla (arrow) (4,45 mbsf). **17-18:** Abnormal specimens with a complex shape characterised by the co-occurrence of different test abnormalities (2,72 mbsf). **19:** Abnormal specimen with a distorted chamber arrangement (10,55 mbsf).

Bars are 100 μm.

Plate 3

Abnormal specimens of *Globigerina bulloides* and *Orbulina universa* throughout the studied record. Note that the stated morphospecies exhibit various morphological abnormalities, often within the same sample. **1-5:** Specimens of *G. bulloides* with abnormal additional chambers or protuberances (6,24 mbsf). **6:** Abnormal specimen of *G. bulloides* with an over-developed chamber (2,72 mbsf). **7-10:** Specimens of *G. bulloides* with abnormal openings(13,08 mbsf). **11:** Specimen of *G. bulloides* with an abnormal chamber morphology (6,00 mbsf)**12:** Abnormal specimen of *G. bulloides* with some traces of test regeneration (arrow) (1,86 mbsf). **13:** Abnormal specimen of *G. bulloides* with a distorted chamber arrangement (2,47 mbsf). **14-20**: Abnormal specimens of *O. universa* with the last chamber reduced in size and that does not include the previous chambers (specimens 14-16 sampled at 10,04 mbsf; specimens 17-20 at 12,72 mbsf). The abnormal specimens are morphologically close to the extinct genus *Praeorbulina* and to the species *Orbulina suturalis*. Bars are 100 μm.

Plate 4

Abnormal specimens of other morphospesies, such as: *Globorotalia trucatulinoides* (left), *Neogloboquadrina incompta, Neogloboquadrina dutertrei, Globigerinita minuta, Globorotalia crassaformis, Globigerinoides elongatus, Globorotalia scitula, Globigerina falconensis, Globigerinita glutinata, Globigerinella* sp. and *Globigerinita uvula* throughout

the studied record. Note that all the stated morphospecies exhibit various morphological abnormalities, often within the same sample.

1-2: Specimens of *G. truncatulinoides* with abnormal additional chambers (6,24 mbsf). **3-6:** Abnormal specimens of *N. incompta* exhibiting different abnormalities as: an abnormal opening (3; at 8,94 mbsf), chambers with a distorted arrangement (4; at 5,60 mbsf)), twinned tests (5; at 14,92 mbsf) and an abnormally protruding chamber (6; at 5,47 mbsf). **7-8:** Specimens of *N. dutertrei* with the last chamber characterised by an abnormal morphology (12,60 and 13,84 mbsf, respectively. **9-11:** Specimens of *G. minuta* exhibiting different abnormalities as: an abnormal additional chamber (9; at 6,11 mbsf) and twinned tests(10-11; at 6,48 mbsf). **12:** Abnormal specimen of *G. falconensis* with an abnormal additional chamber (2,72 mbsf). **13-14:** Abnormal specimens of *G. elongatus* with abnormal additional chambers (15,16 and 13,08 mbsf, respectively). **15:** Abnormal specimen of *G. scitula* with an abnormal additional chamber (7,09 mbsf). **16:** Abnormal specimen of *G. crassaformis* with an abnormal additional chamber (10,04 mbsf). **17:** Abnormal specimen of *G. glutinata* with an abnormal additional chamber (5,47 mbsf). **18:** Abnormal specimen of *Globigerinella* sp. with an abnormal additional chamber (11,68 mbsf). **19-20:** Abnormal specimens of *G. uvula* with abnormal additional chambers (15,96 mbsf). Bars are 100 μm.

Plate 5

Different categories of morphological abnormalities recorded in the core IMAGES MD 97-2114. These categories are inspired by the paper of Geslin (2000). See the text for further explanations.

SUPPLEMENTARY DATA (ONLY ON-LINE)

Table A. Total census of the studied planktonic foraminiferal assemblages

Table B. Subdivision of the counted abnormal specimens of each morphospecies within the different categories of abnormality here labelled with the alphabetical letters from A to I. Note that each morphospecies exhibits different categories of abnormality generally within the same sample.

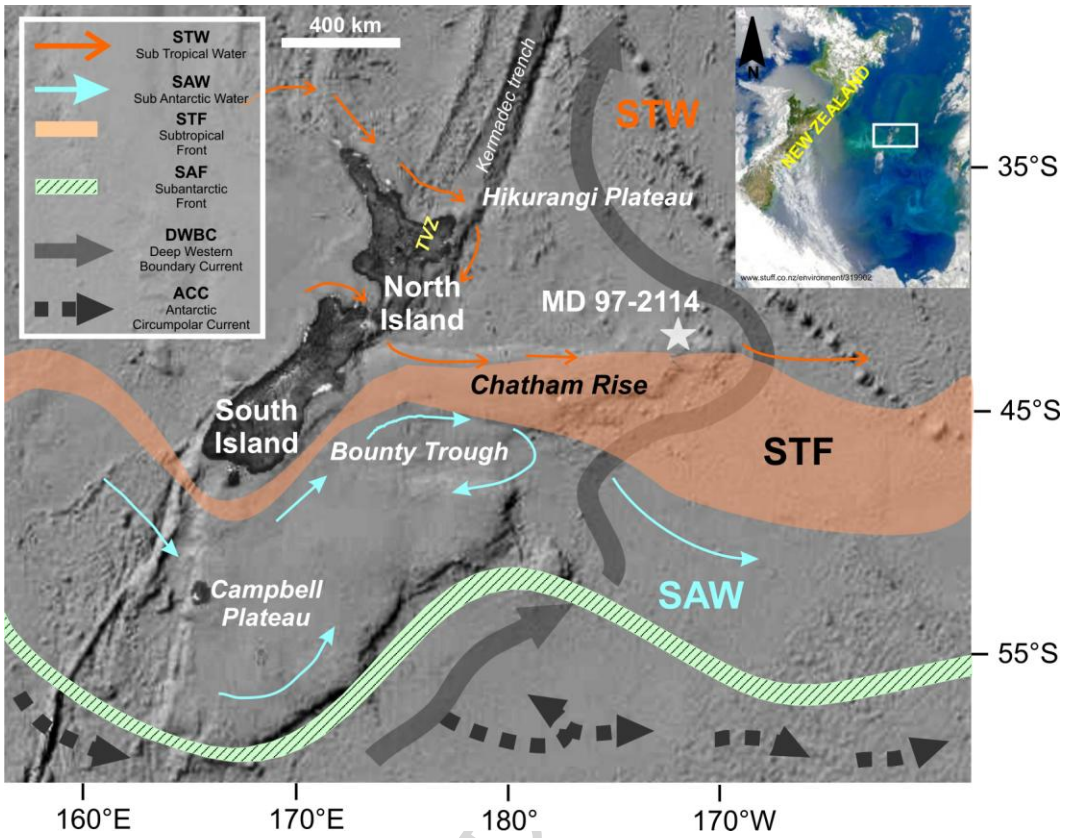

Figure 1

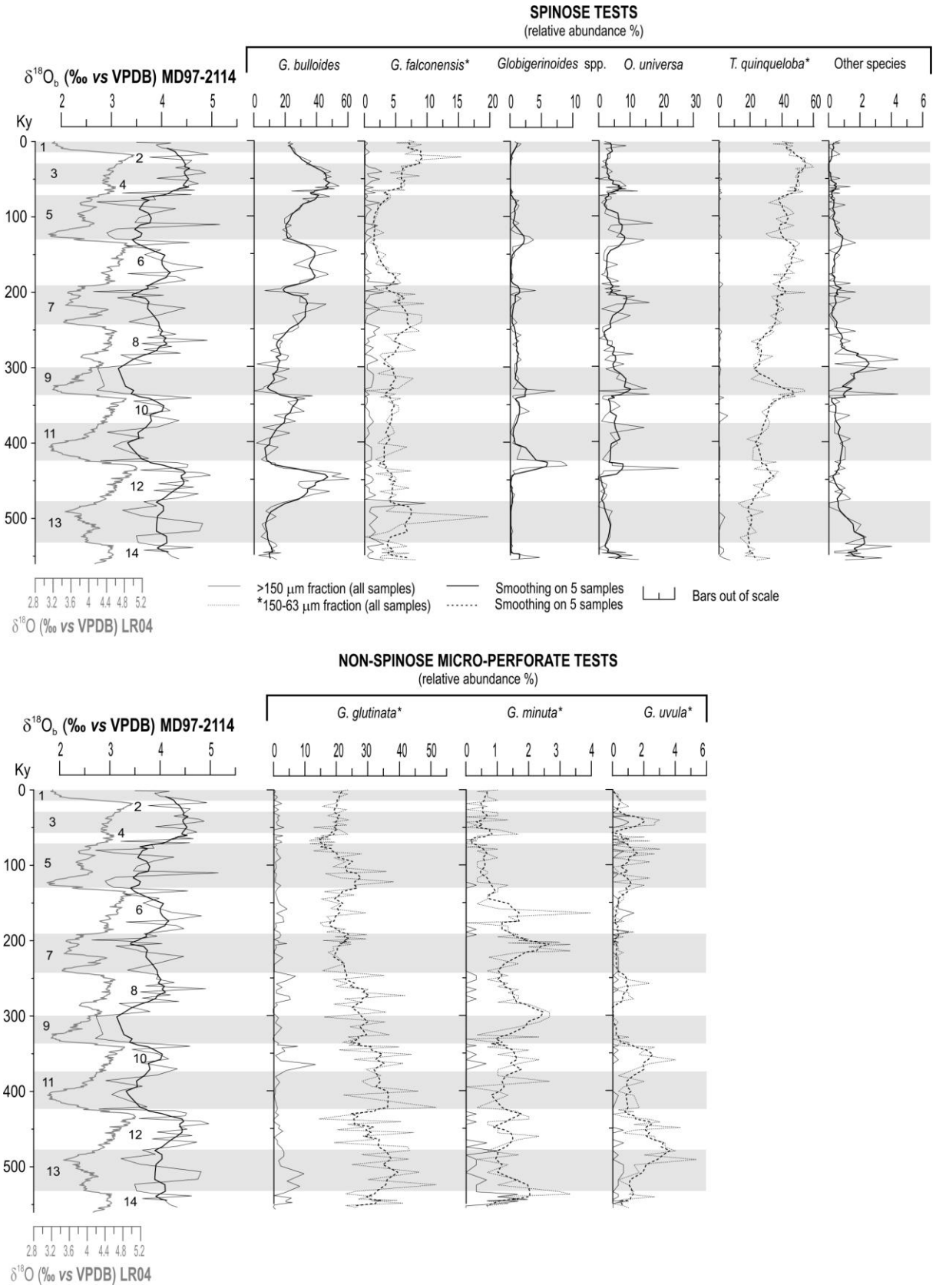

Figure 2A

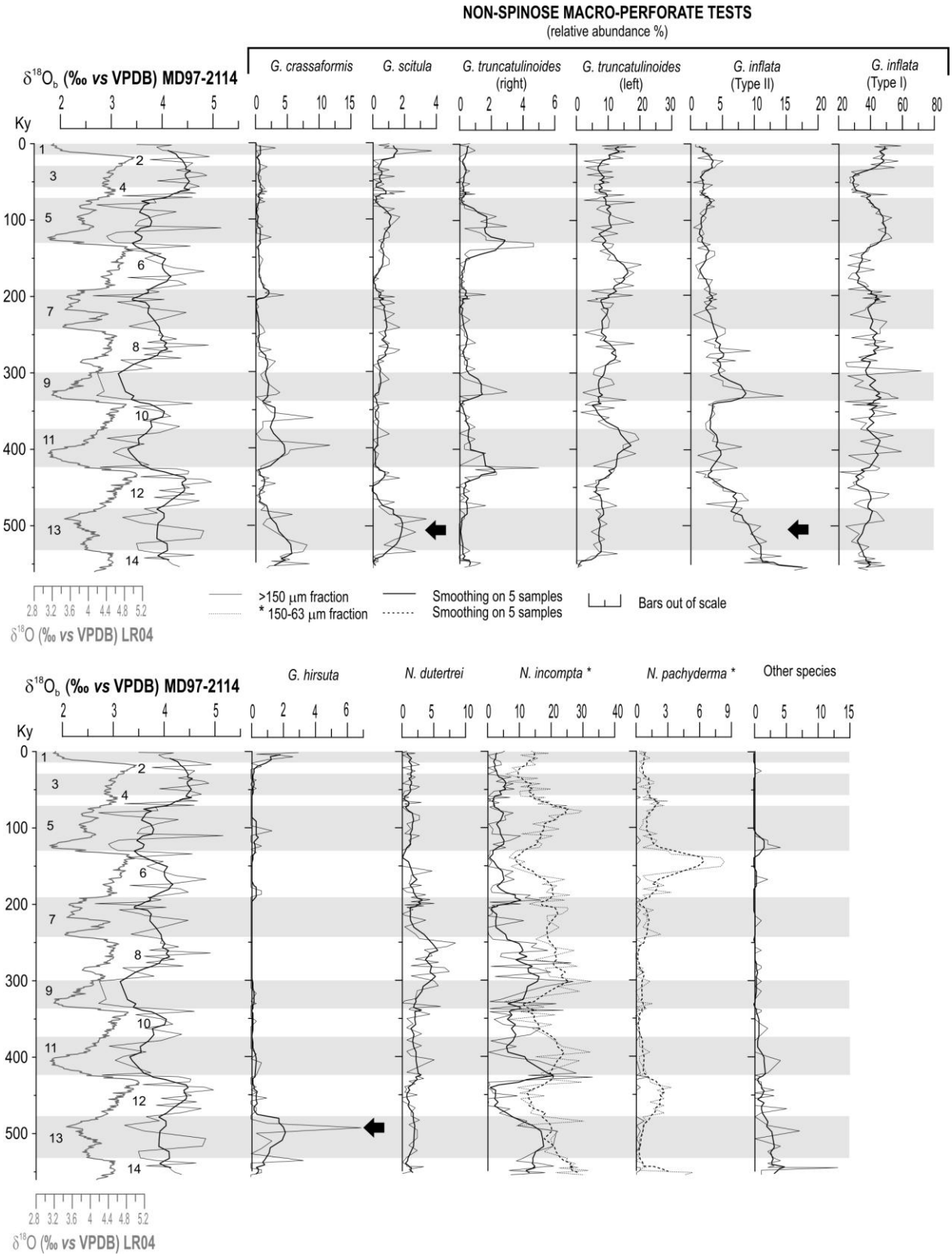

Figure 2B

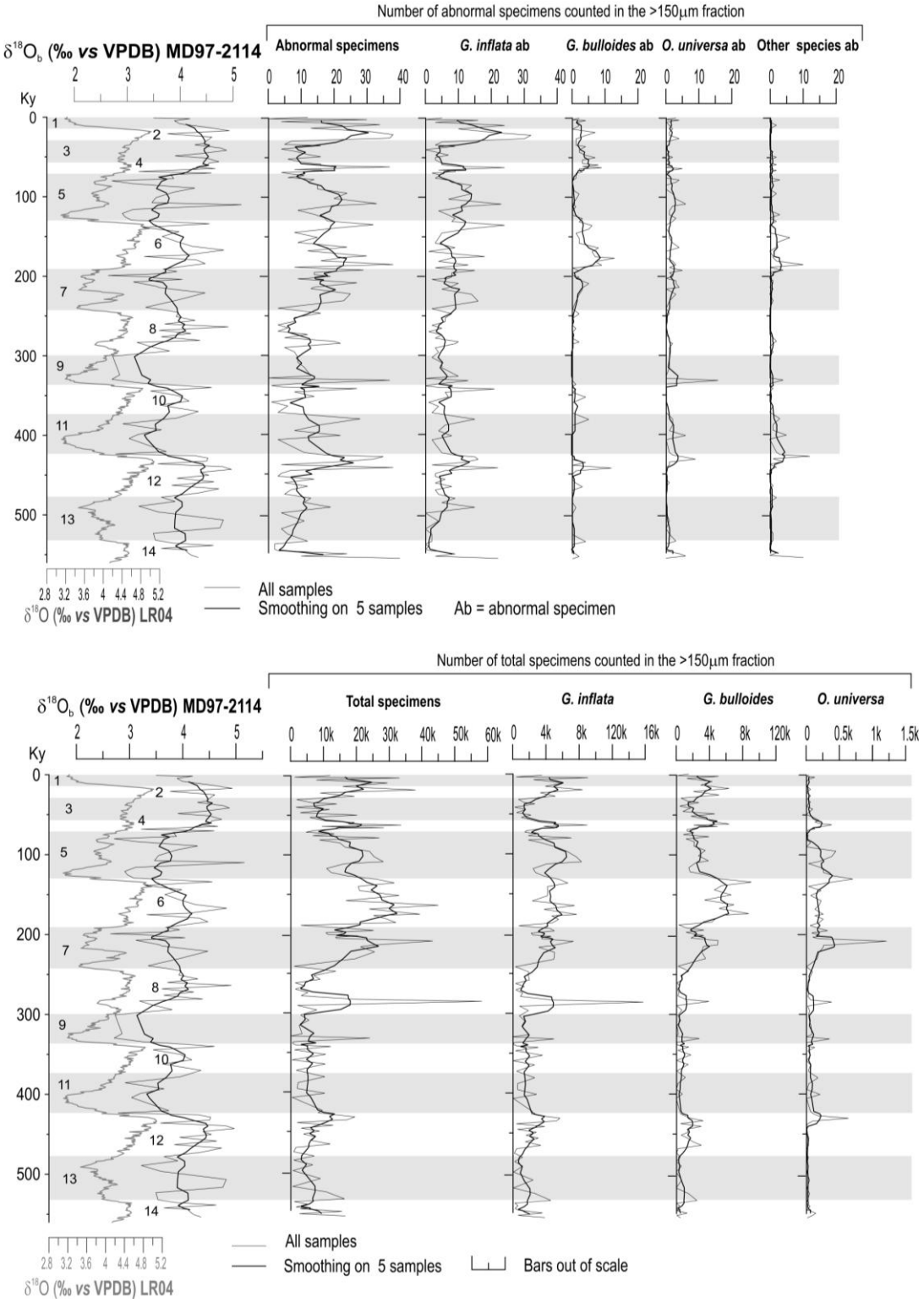

Figure 3

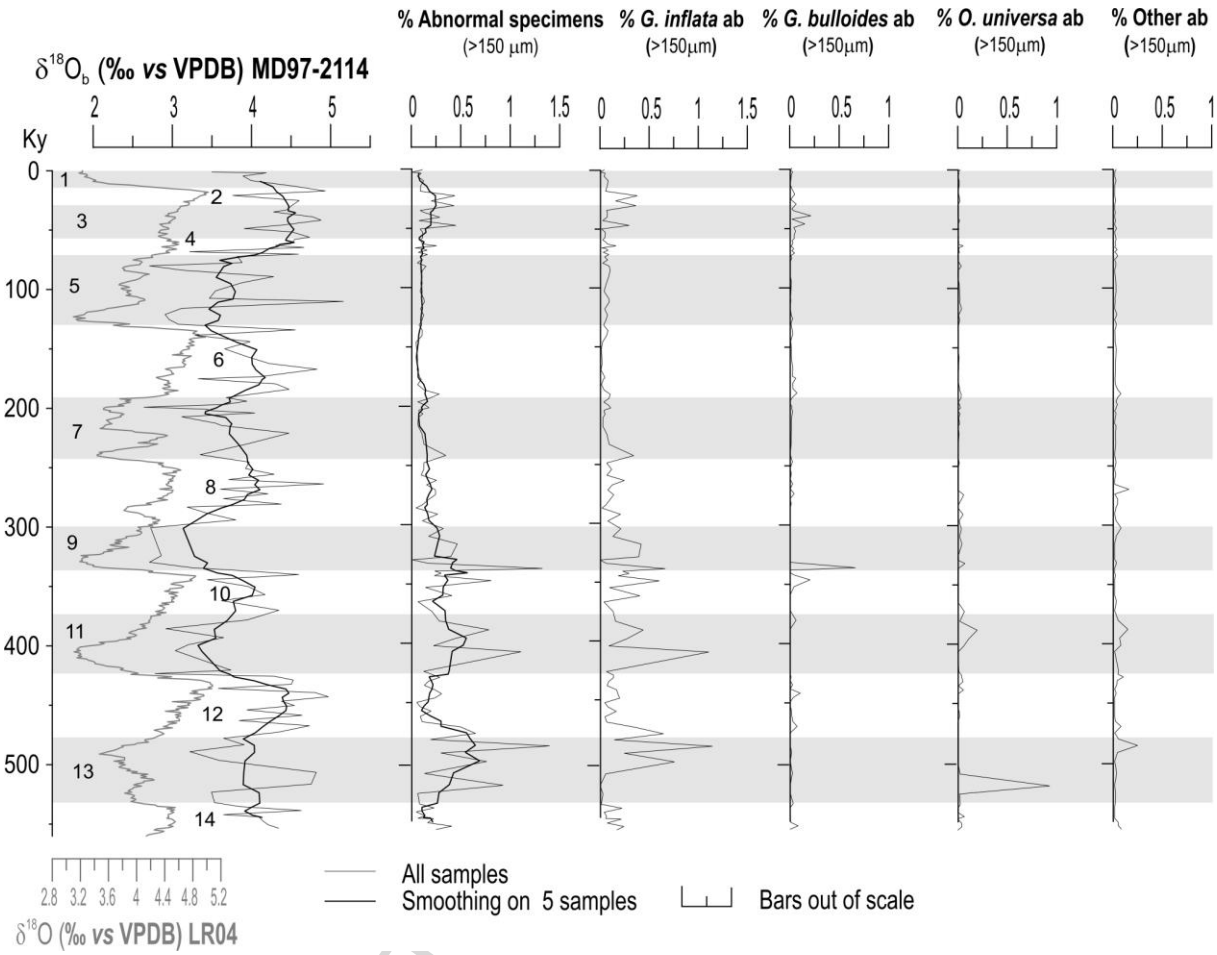

Figure 4

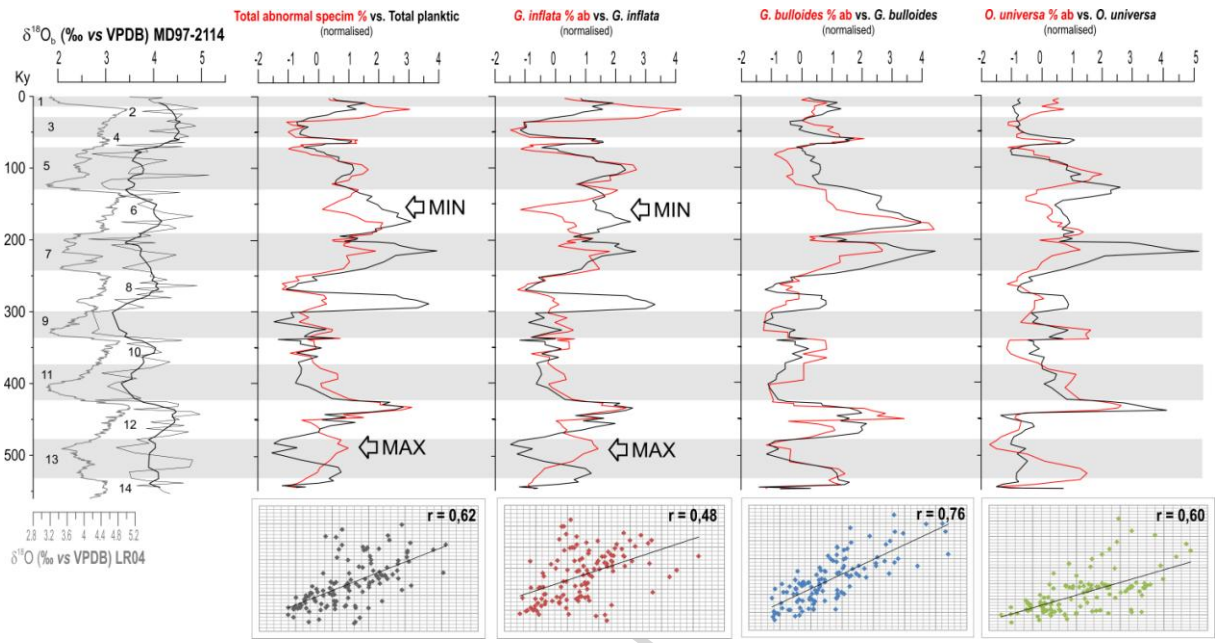

Figure 5

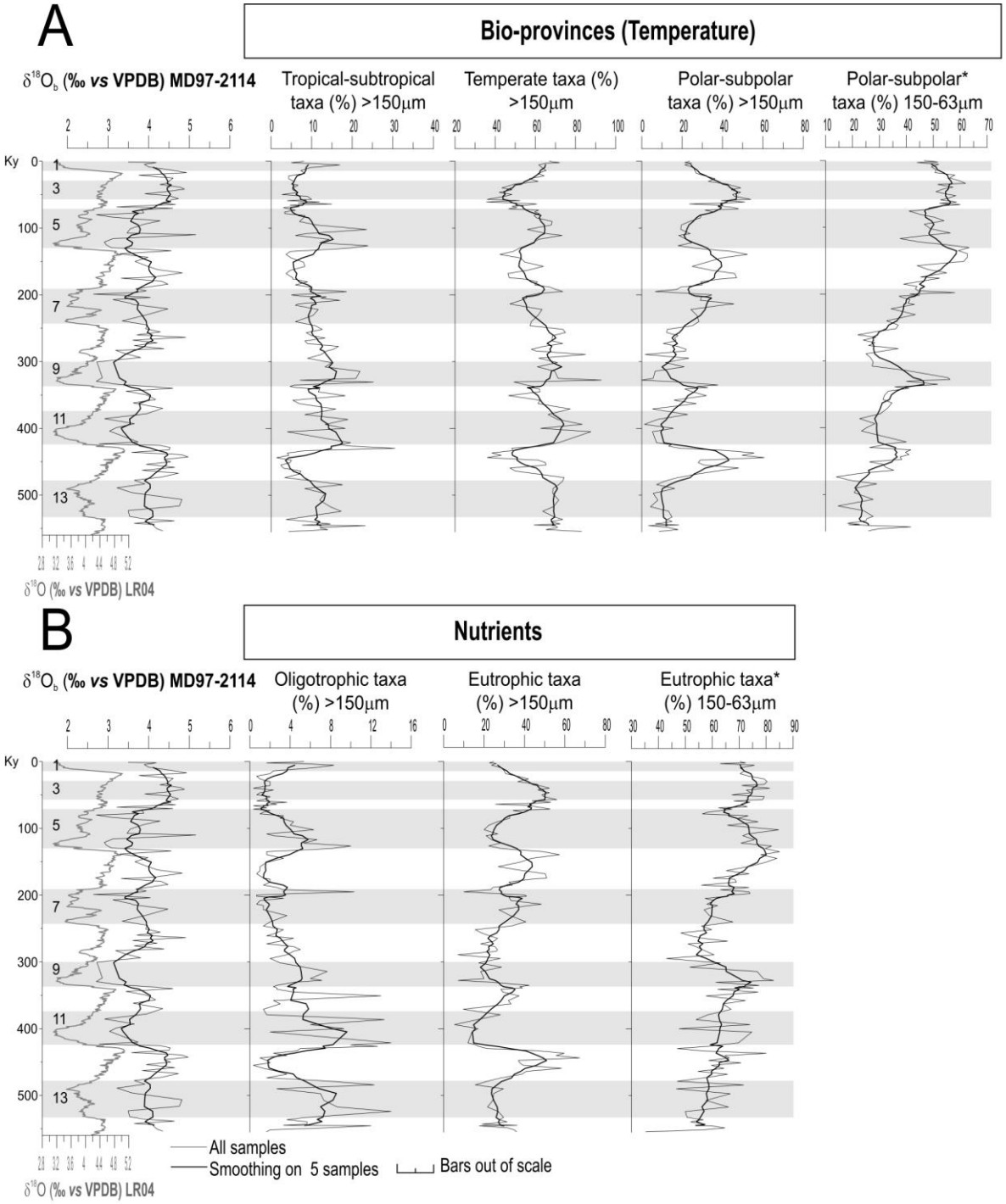

Tropical-subtropical taxa: *Globigerinoides* spp., *O. universa*, *N. dutertrei*, *G. hirsuta*, *G. scitula*, *G. crassaformis*, *G. truncatulinoides* dx
Temperate taxa: *G. falconensis*, *N. incompta*, *G. inflata* (Type I), *G. truncatulinoides* sx
Polar-subpolar taxa*: *G. bulloides*, *T. quinqueloba*, *N. pachyderma*
Eutrophic taxa*: *G. bulloides*, *T. quinqueloba*, *G. glutinata*, *N. pachyderma*, G. i*nflata* (Type II)
Oligotrophic taxa: *Globigerinoides* spp., *G. hirsuta*, *G. scitula*, *G. crassaformis*, *G. truncatulinoides* dx
*Since *T. quinqueloba*, *N. pachyderma* and *G. glutinata* are mostly small-size species in the studied record, data were integrated by the use of the 150-63 μm fraction

Figure 6

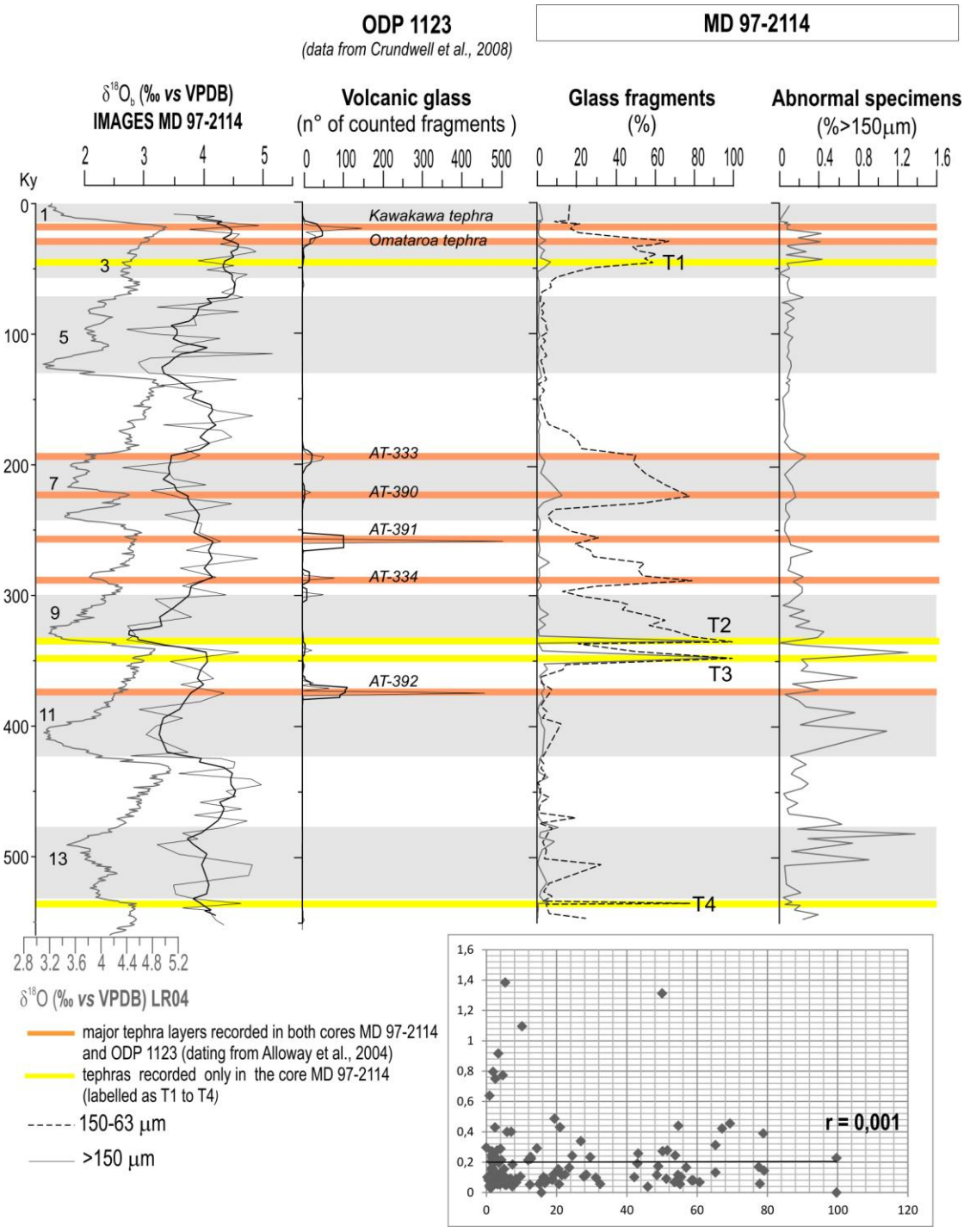

Figure 7

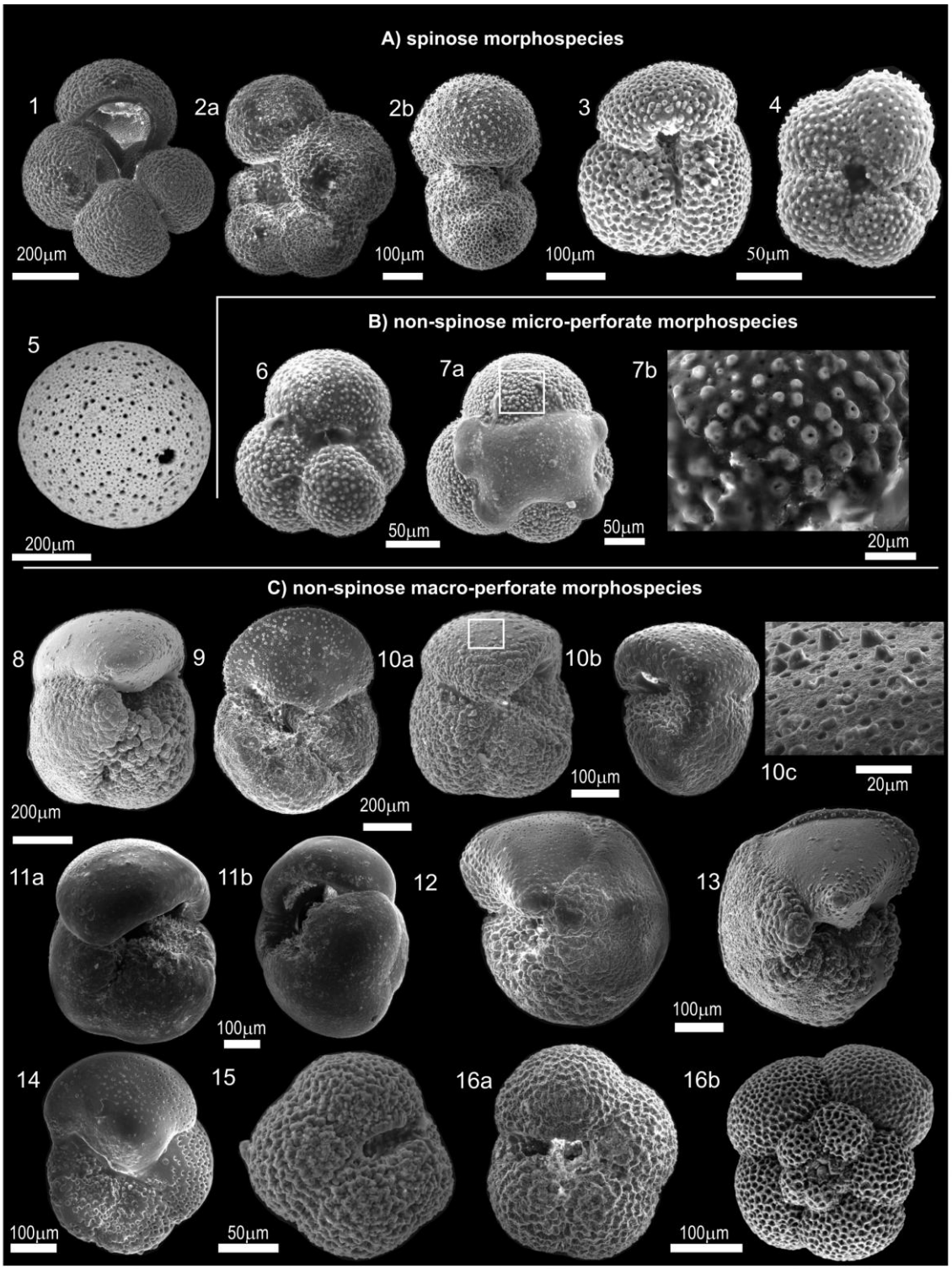

Plate 1

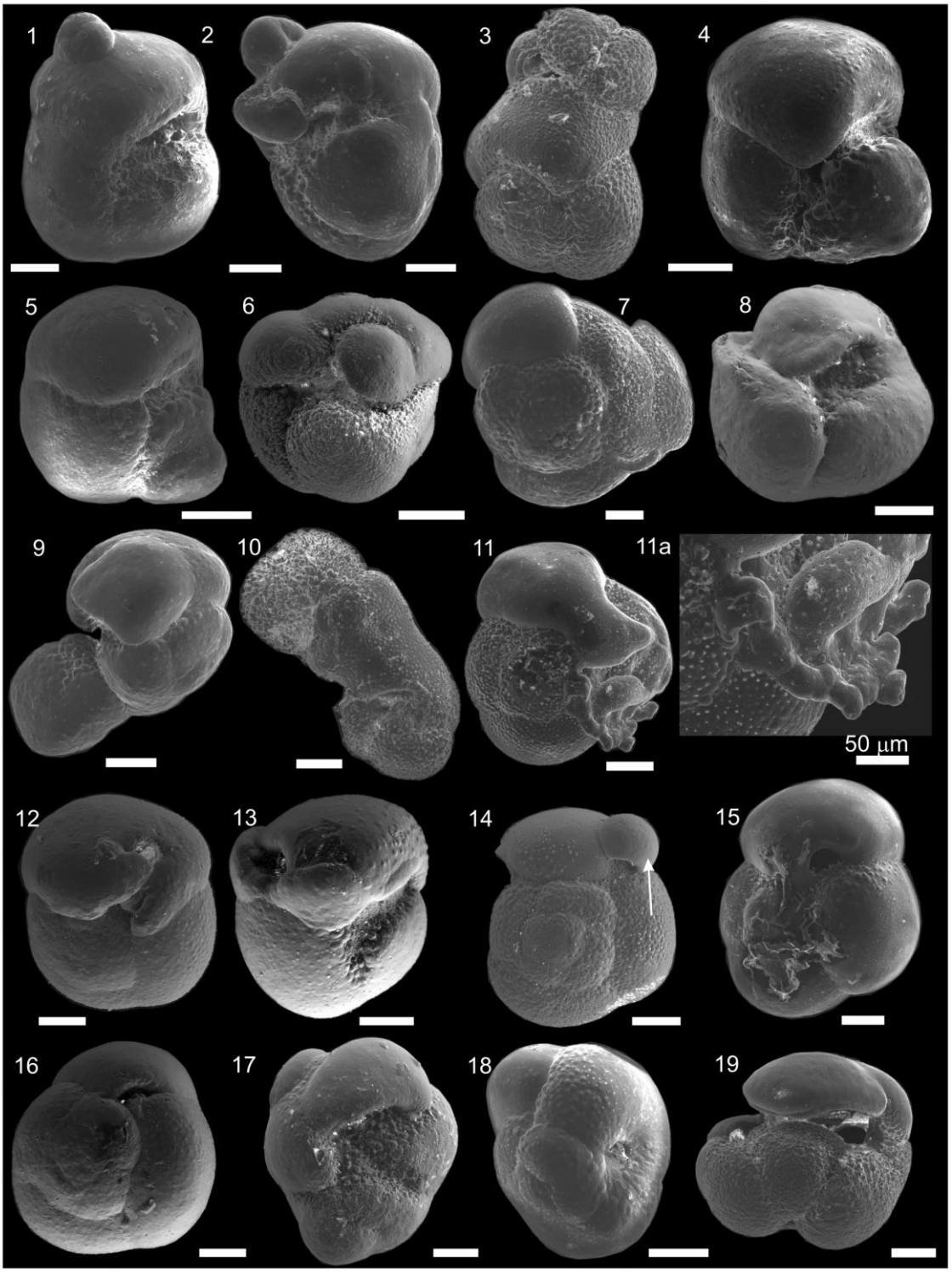

Plate 2

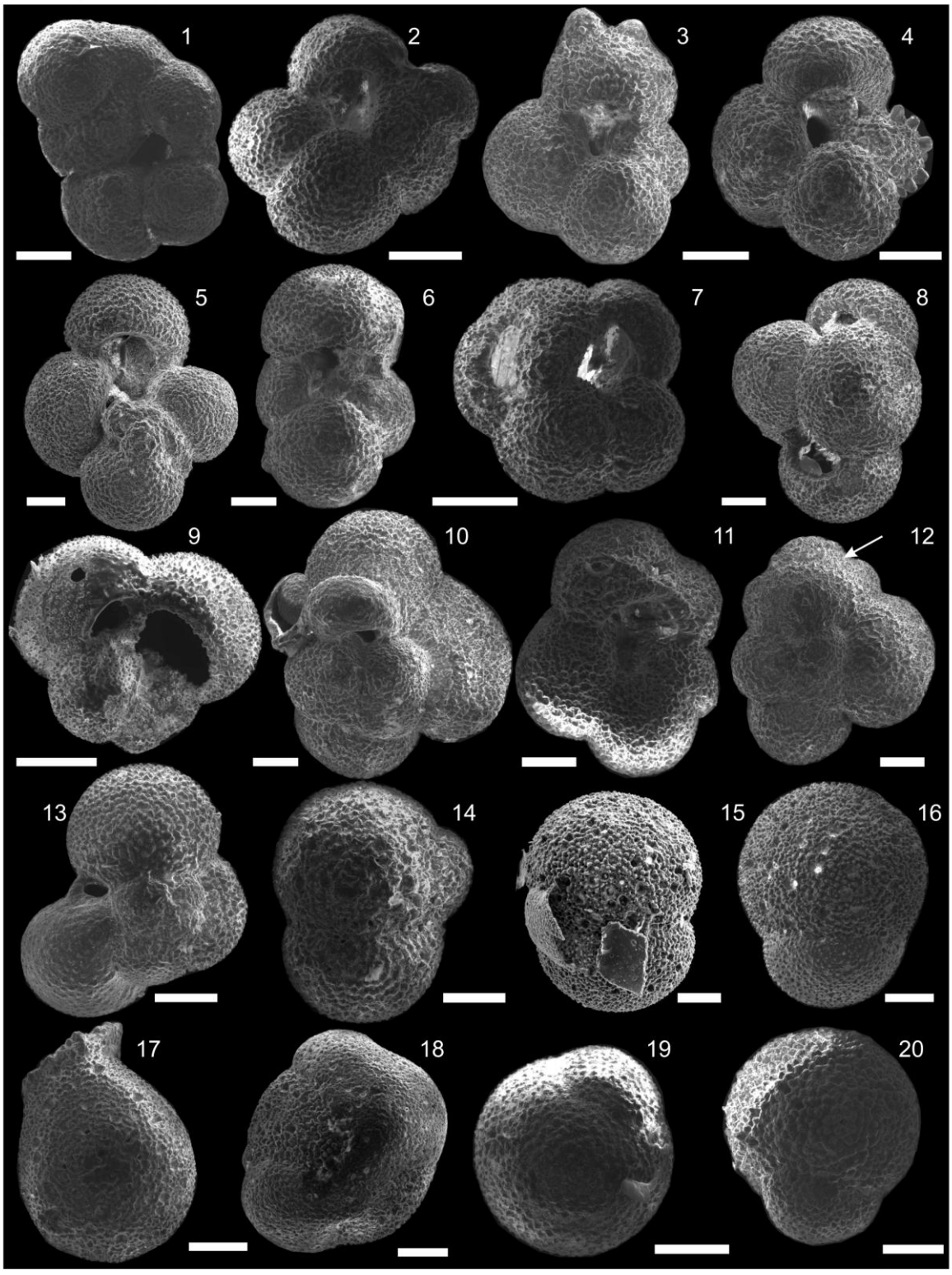

Plate 3

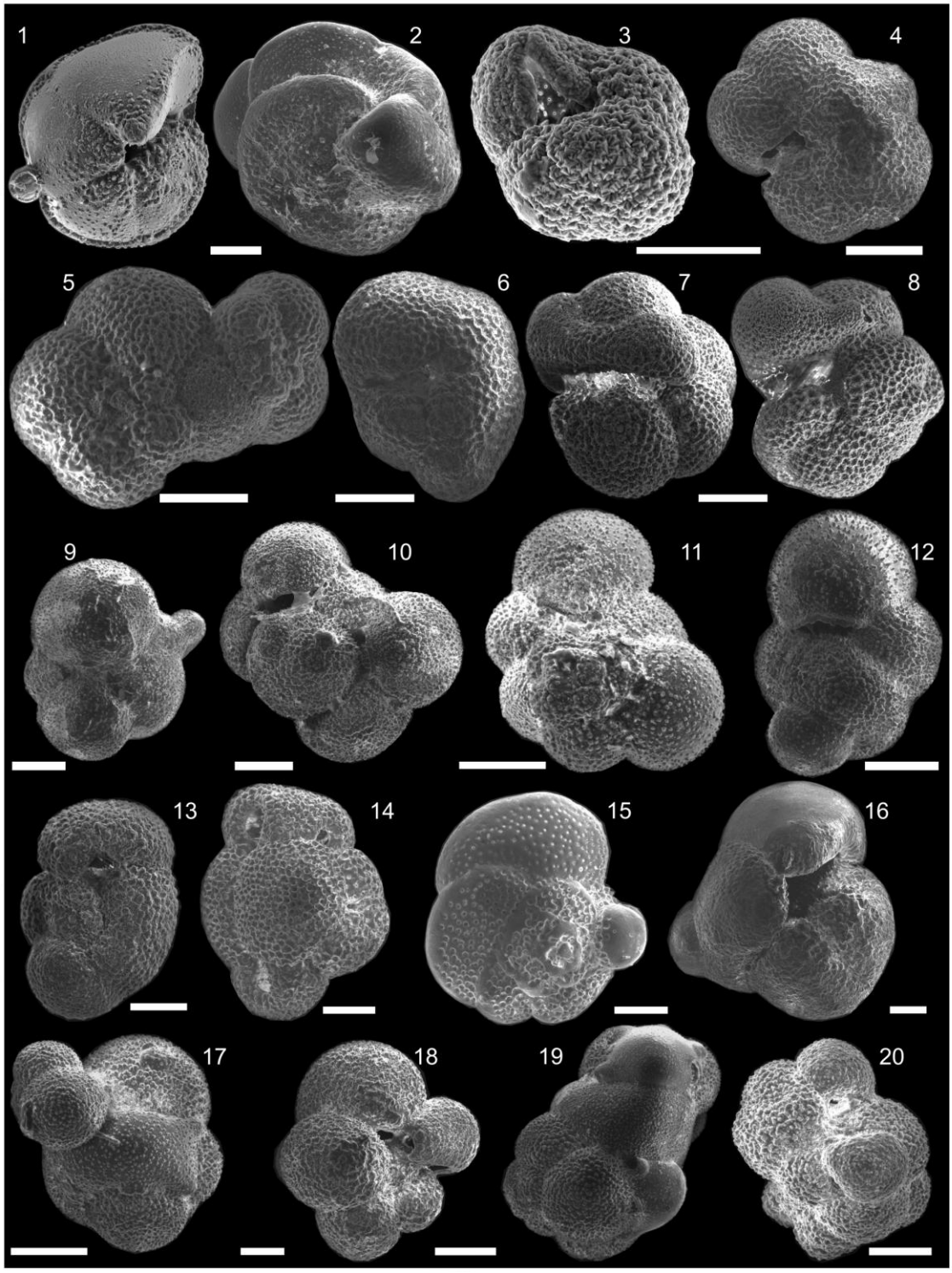

Plate 4

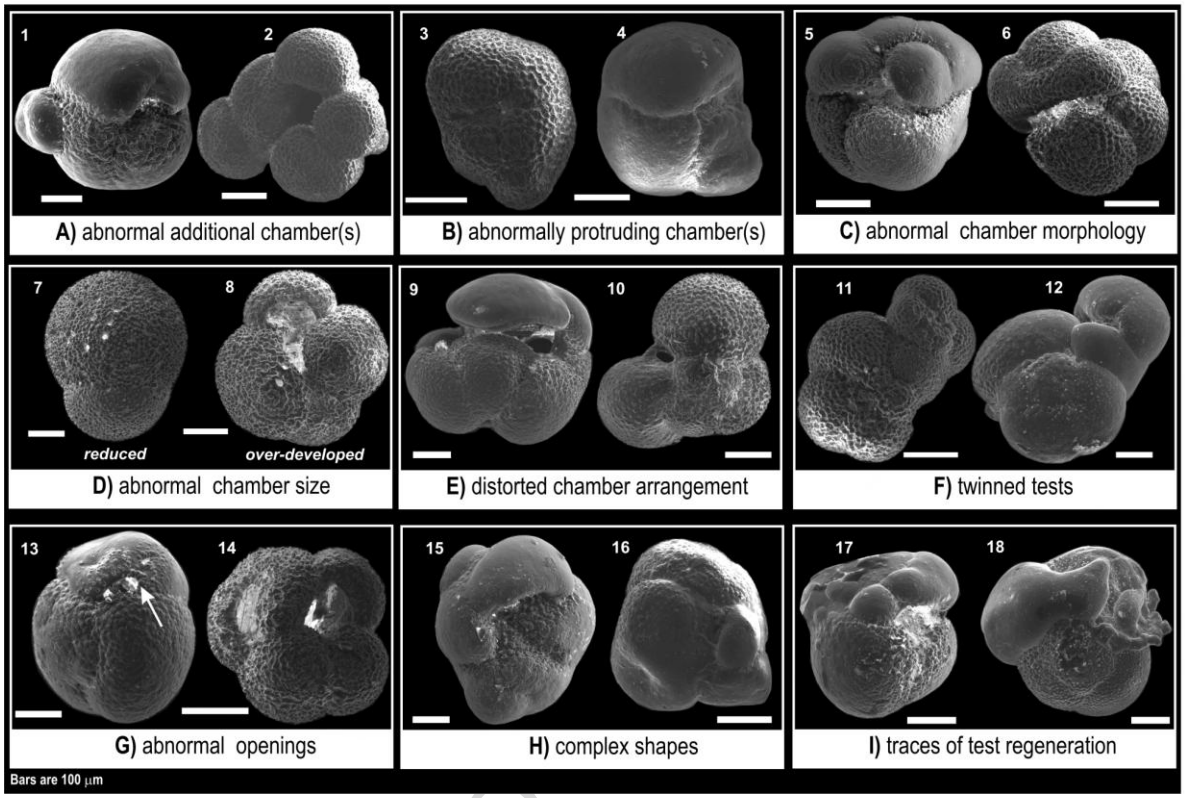

Plate 5

Table 1

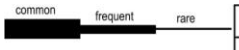

		Bio-provinces					Depth (m)			Nutrients			Water masses		remarks	Ref.
		Polar	Subpolar	Temperate	Subtropical	Tropical	>100	45-100	0-45	Oligo.	Meso.	Eu.	stratified	mixed		
Spinose species	*Globigerina bulloides*							X				X		X	Common in up-welliimg areas with high nutrients. It lacks photosymbionts	2,4,5,6
	Globigerina falconensis								X							2,6,9
	Globigerinella siphonifera								X	X					Can tollerate high salinity variations. The temperate forms need a major nutrient supply (mesotrophy).	4,6
	Globigerinoides conglobatus								X	X					Less abundant then *G. ruber* and *G. sacculifer*	2,4,6
	Globigerinoides ruber								X	X					Two phenotypes: "white" more abundant and "pink" less abundant. This last prefers higher SST°.	1,2,4,6,10
	Globigerinoides sacculifer								X	X					Can tollerate high salinity variations.	2,4,6
	Orbulina universa								X		X			X	Test size related to T° and nutrient supply. Major abundances in up-welling regions with strong surface currents	4,6
	Turborotalita quinqueloba								X			X		X		2,4,5,6
	Hastigerina pelagica							X							Carnivorous, lacking photosymbionts	2,5,6
Non-spinose macro-perforate species	*Globorotalia crassaformis*						X			X	X		X		Rare living specimens.	2,4,5,6,9
	Globorotalia hirsuta						X			X			X			
	Globorotalia inflata (type II)											X		X	Since ca. 700Ka, morphotype limited to the subpolar areas.	6,7
	Globorotalia inflata (type I)						X			X	X				Common in the southern margin of the STW.	2,5,6,7
	Globorotalia menardii						X			X			X		Missing in the studied samples	4,6,9
	Globorotalia scitula						X			X			X			4,6
	Globorotalia truncatulinoides (right)						X			X			X			2,4,5,6,8
	Globorotalia truncatulinoides (left)						X				X		X		In the southern emisphere the left-coiling specimens increase in abundance with latitude	2,4,5,6,8
	Neogloboquadrina dutertrei														Chambers increase in number from temperate to tropical areas. It characterises low-salinity surface waters with *G. ruber*	4,6,10
	Neogloboquadrina pachyderma								X			X		X	Can tollerate very high salinities >82pmu. Con occur in tropical-subtropical up-welling	2,3,4,5,6
	Neogloboquadrina incompta															2,3,4,5,6
Non-spinose micro-perforate	*Globigerinita glutinata*											X				2,4,6
	Globigerinita minuta											X(?)			Ecologically similar to *G. glutinata*.	2,6
	Globigerinita uvula															4,6

1) Aurahs et al., 2011; **2)** Crundwell et al., 2008; **3)** Darling et al., 2006; **4)** Darling & Wade, 2008; **5)** Hayward et al., 2012; **6)** Hemleben et al., 1989; **7)** Morard et al., 2011; **8)** Ujiié et al., 2010; **9)** Kucera et al., 2005; **10)** Ufkes et al., 1998.

Highlights

- The studied planktonic foraminifera developed abnormal tests throughout the entire 550ka record
- Abnormal tests have percentages not exceeding 1.5% of the total planktonic assemblage
- Test abnormalities mostly occur in the morphospecies *G. inflata*, *G. bulloides* and *O. universa*
- Test abnormalities occur with a long-term decreasing trend up core
- The highest percentages of abnormalities are recorded during interglacials MIS 13, 11 and 9